ECN

Energy research Centre of the Netherlands

EOSLT Consortium Biomass Co-firing

WP 4 - Biomass co-firing in oxy-fuel combustion
Part I: Lab- Scale Experiments

L. Fryda

ECN-E--10-079 JULY 2010

Acknowledgement/Preface
The research work reported in this report was carried out in the frame of EOSLT Consortium Biomass Co-firing with partial financial support from the two RFCS projects: RFCR – CT – 2006 – 00010 (BOFCOM) and RFCR-CT-2007-00009 (ECOSCRUB).

Abstract
In the frame of WP4 of the EOS LT Co firing program, the ash formation and deposition of selected coal/biomass blends under oxyfuel and air conditions were studied experimentally in the ECN lab scale coal combustor (LCS). The fuels used were Russian coal, South African coal and Greek Lignite, either combusted separately or in blends with cocoa and olive residue. The first trial period included tests with the Russian and South African coals and their blends with cocoa, the second trial period included Lignite with olive residue tests and a final period firing only Lignite and Russian coal, mainly to check and verify the observed results. During the testing, also enriched air combustion was applied, in order to establish conclusions whether a systematic trend on ash formation and deposition exists, ranging from conventional air, to enriched air (improving post combustion applications) until oxyfuel conditions. A horizontal deposition probe equipped with thermocouples and heat transfer sensors for on line data acquisition, and a cascade impactor (staged filter) to obtain size distributed ash samples including the submicron range at the reactor exit were used. The deposition ratio and the deposition propensity measured for the various experimental conditions were higher in all oxyfuel cases. No significant variations in the ash formation mechanisms and the ash composition were established. Finally the data obtained from the tests performed under air and oxy-fuel conditions were utilised for chemical equilibrium calculations in order to facilitate the interpretation of the measured data; the results indicate that temperature dependence and fuels/blends ash composition are the major factors affecting gaseous compound and ash composition rather than the combustion environment, which seems to affect neither the ash and fine ash (submicron) formation, nor the ash composition. The ash deposition mechanisms were studied in more detail in Part II of this report.

Contents

List of tables

List of figures

Nomenclature and list of symbols

SEM/EDS	Scanning Electron Microscopy / Energy Dispersive Spectroscopy
ICP/AES	Inductively Coupled Plasma / Atomic Emission Spectroscopy
K, Cl, S, Si	Potassium, Chlorine, Sulphur, Silicon
ADP	Ash Deposition Predictor
CCS	Carbon Capture and Sequestration
USC	Ultra Supercritical Combustors
IPCC	Intergovernmental Panel on Climate Change
ZET	Zero Emission Technology
ASU	Air Separation Unit
RFG	Recirculation Flue Gas
EOR	Enhanced Oil Recovery
PC/PF	Pulverised Coal/Fuel
CFD	Computational Fluid Dynamics
XRD	X ray Diffraction
LCS	Lab-scale Combustion Simulator
DP	Deposition Propensity (%)
DR	Deposition Ratio (-)
ppm	Parts Per Million
Rf	Fouling Factor
EF	Enrichment Factor

Summary

Combustion in an O_2/CO_2 mixture (oxyfuel combustion) has been recognized as a promising technology for CO_2 capture as it produces a high CO_2 concentration flue gas. Furthermore, biofuels in general contribute to CO_2 reduction in comparison with fossil fuels as they are considered CO_2 neutral. Ash formation and deposition (surface fouling) behaviour of coal/biomass blends under O_2/CO_2 combustion conditions is still not extensively studied. In the frame of WP4 of the EOS LT Co firing program, the ash formation and deposition of selected coal/biomass blends under oxyfuel and air conditions were studied experimentally in the ECN **L**ab scale **C**ombustor **S**imulator (LCS). The fuels used were Russian and South African coal, and Greek Lignite either combusted separately or in blends with cocoa and olive residues. The tests were carried out in several testing periods: (1) first carrying our tests with the Russian and South African coals and their blends with cocoa, then (2) the Lignite with olive residue tests followed and (3) a final period firing only Lignite and Russian followed, in order to check and verify the observed results. During the second test series, an additional combustion environment was applied, namely enriched air conditions, in order to establish conclusions on a systematic trend on ash formation and deposition, ranging from conventional air, to enriched air (improving post combustion applications) until oxyfuel conditions. A horizontal deposition probe, equipped with thermocouples and heat transfer sensors for on line data acquisition, was placed at a fixed distance from the burner in order to simulate the ash deposition on heat transfer surfaces (e.g. water or steam tubes). Furthermore, a cascade impactor (staged filter) was used to obtain size distributed ash samples including the submicron range at the reactor exit. The deposition ratio and propensity measured for the various experimental conditions were higher in all oxyfuel cases. The SEM/EDS and ICP analyses of the deposit and cascade impactor ash samples indicate K interactions with the alumina silicates and to a smaller extend with Cl, which was all released in the gas phase, in both the oxy-fuel and air combustion samples. Sulphur was depleted in both the air or oxyfuel ash deposits. Initially, S and K enrichment was detected in the fine ash stages, slightly increased under air combustion conditions, but this result was not reproduced therefore conclusions cannot be drawn. Finally the experimental data obtained from the tests performed under air and oxy-fuel conditions were utilised for (a) chemical equilibrium calculations and (b) ash deposition modelling study using the Ash Deposition Predictor (ADP), developed and implemented by ECN, in order to obtain insight to the observed results and gain knowledge on the parameters that affect the ash formation and deposition mechanisms under varying combustion conditions. The chemical equilibrium calculation results indicate that temperature dependence and fuels/blends ash composition are the major factors affecting gaseous compound and therefore ash composition instead of the combustion environment (air vs. oxyfuel), which does not seem to affect neither the ash and fine ash (submicron) ash formation, nor the ash composition. The ADP results, shown and commented upon in Part II of the report, give some interesting information on the parameters affecting the observed deposition behaviour, as it takes into account the physical properties of the gaseous flows and the ash particles, without considering chemical interactions, as opposed to the chemical equilibrium calculations.

1. Introduction

Combustion in O_2/CO_2 mixture (oxy-fuel) has been recognised as a promising technology for CO_2 capture as it produces a high CO_2 concentration flue gas [1-7]. This technology is based on fuel combustion in a mixture of oxygen, produced in an Air Separation Unit, and recirculated flue gas. Oxy-fuel combustion and flue gas scrubbing (to separate the CO_2 from the combustion products using amines) are technologies that can be retrofitted to existing units. Including biomass co-firing in the oxyfuel concept, helps achieving even negative net emissions, which will increase further the political and public support for Carbon Capture and Sequestration (CCS). Biomass co-firing can address the technical CCS challenges with different percentages of biomass co-fired, according to the Zero Emission Platform reports on the current status of the oxyfuel technology [8], however some technological blocks still need to be fully validated prior to proceeding with commercialising the technology. One of these technology blocks that need validation and further Research and Development is the oxyfuel combustion process itself, including fuel preparation and including biomass co firing. At the same level lies the fuel recycling issue, including the level of gas cleaning necessary to allow for problem free boiler operation. The overall process integration, e.g. heat stream matching as well as advanced boiler materials for Ultra Supercritical Combustors (USC) operation are also still subject to research and development, in order to validate the concept. In this frame, targeted lab scale tests are an easy and fast way to gather information and hints on how to proceed in the pilot scale. More experimental results in different lab scale installations are necessary to identify problems, if existing, and propose counteractions, and also try a wide variety of fuels and combustion conditions, parameters that are impossible to alter easily in the pilot and large scale.

The integration of biomass in the oxyfuel co-firing blend has not yet been studied extensively and there are open questions prior to utilising biomass under oxyfuel conditions, as for example, the ignition of blends under oxyfuel conditions, proper temperature conditions, the degree of flue gas cleaning prior to recirculation, the effect of biomass ash components under CO_2 and increased O_2 conditions or the behaviour of ash deposition under varying gaseous environment. The flue gas enrichment in S and Cl due to the necessary recirculation can affect the ash formation and deposition, inducing further ash melting and enhancing the fine ash particle formation.

The aim of the work reported is the comparative study of ash formation and deposition of selected coal/biomass blends under oxyfuel and air conditions in the Lab scale Combustor Simulator (LCS) for pulverized fuels. The fuels used were Russian and South African coals as well as Lignite, and selected blends at 20 % w/w with cocoa and olive residue. Ash samples were subjected to SEM/EDS and ICP analyses and chemical equilibrium calculations using FACTSage® were carried out to facilitate the interpretation of the ash composition related data. In addition, ash deposition modelling study using the Ash Deposition Predictor (ADP), developed and implemented by TU Delft and ECN, was implemented in order to obtain insight to the observed results and gain knowledge on the parameters that affect mainly the ash deposition under varying combustion conditions. The results of this work however will be presented in a separate report.

2. Literature review and state of the art

2.1 Review of oxygen combustion technologies and state of the art in research

The scope of this study is to collect the knowledge on the ongoing activities in both the European and worldwide market and the state of the art of the technologies for emissions minimization, in combination with the partial substitution of coal with biomass. Furthermore, an effort is made to evaluate the technologies, based on the available literature, considering the thermal conversion process that takes place in the boiler, the emission level control and minimization potential and the specific characteristics of biomass as secondary fuel. The combination of these technologies is expected to exclude some options that apply to exclusively one technology, given the fact that there are certain limits and requirements to be fulfilled in every case separately.

2.1.1 Zero or near zero emission technologies

The Zero Emission Technology (ZET) term is mainly used to describe CO_2 emission abatement; greenhouse gas emissions in general can be decreased through increased power plant energy efficiency, use of lower carbon-intensive fuels and greater use of renewable energy, and through CO_2 capture technologies. Highly efficient power plants with near-zero emissions will drastically reduce the environmental impact of fossil fuel use. Technological advances though should focus on the combined and simultaneous reduction of all pollutant emissions, such as SO_2, NO_x, particulates and Hg, in parallel to CO_2 and other greenhouse gas emissions. A variety of advanced technologies are available to enhance the environmental performance of power plants; any improvement in the environmental performance of coal plants will increase the likelihood that electricity generation from coal will continue in the long-term.

A simple method to reduce CO_2 immediately is co firing of fossil fuels with biomass, which at the same time saves significant amounts of fuels. Emission reduction methods involve treatment of the flue gas after combustion and can therefore be applied to any of the conventional as well as advanced power production technologies, with or without co-firing. Advanced power plant technologies aim towards the improvement of the efficiency and therefore reduce emissions indirectly. Advanced clean coal conversion technologies include Supercritical Pulverised Coal Combustion (PCC), Circulating Fluidised Bed Combustion (CFBC), Pressurised Fluidised Bed Combustion (PFBC), Integrated Gasification Combined Cycle (IGCC), for the short to medium term needs, and concerning the new plant construction, PCC with supercritical as well as sub critical conditions. Supercritical PCC and IGCC based on various gasification technologies provide the main basis for ZETs, adapting further reduction of emission technologies of conventional emissions (SO_2, NOx, particulates, Hg, CO_2).

Table 2.1 summarises the targets for ZETs for some power generation technologies as presented in the IPCC Special Report on Carbon Dioxide Capture and Storage [2]. In the case of CO_2 capture, the flow of flue gas volume per fuel consumed is reduced, relative to air-fired combustion, therefore the expression for the emissions based on volume or mass concentration of pollutants in flue gas has to change in order to set a common basis for comparison, beside the fact that theoretically there will be no stack gas release to the atmosphere.

The IPCC Report [2] reviews the current state of the art for processes concerning emissions reduction. For power plants, current commercial CO_2 capture systems can reduce CO_2 emissions by 80−90% / kWh (85−95% capture efficiency). The cost of electricity production increases for a similar type of plant without capture, corresponding to a 40−85% increase for a supercritical pulverized coal (PC) plant, 35−70% for a natural gas combined cycle (NGCC) plant and 20−55% for an integrated gasification combined cycle (IGCC) plant using bituminous coal. These costs include CO_2 compression but not additional transport and storage costs. The lowest CO_2 capture costs were found for industrial processes such as hydrogen production plants that produce concentrated CO_2 streams as part of the current production process; such industrial processes may represent some of the earliest opportunities for CO_2 Capture and Storage (CCS).

In all cases, CO_2 capture costs are dependent on technical, economic and financial factors related to the design and operation of the production process or power system of interest, as well as the design and operation of the CO_2 capture technology employed. Thus, comparisons of alternative technologies or CCS cost estimates require a specific context to be meaningful. New or improved methods of CO_2 capture, combined with advanced power systems and industrial process designs, can significantly reduce CO_2 capture costs and associated energy requirements.

Table 2.1 *Emissions & suggested targets for ZETs for power generation technologies (stack gas concentrations @ 6% O_2, dry) [2]*

Technology*	**SO_2 emissions (mg/m^3)**	**NO_x emissions (mg/m^3)**	**Particulates (mg/m^3)**	**Hg**	**CO_2, kg/kWh_e**
PCC+FGD	100 - 400 (90-98% removal)	100-200 (SCR)	10-15		710-920
CFBC	(90 -98% removal)	<200-400	<50		
PFBC	(90 -98% removal)	120-400	<50		
IGCC	(90 -99% removal)	<75	<1		
NGCC	-	<30 (SCR) – 300	0		~370
PCC target ZETs	<100 interim(2015) <30 eventually	<100 interim (2015) <50 eventually	<10	90% removal	>80% removal
Oxy coal PCC target ZCCs	No stack gas	No stack gas	No stack gas	90% removal No stack gas	No stack gas
IGCC target ZCCs	<25	<25	<1	90% removal	> 80% removal

* PCC Pulverised Coal Combustion
FGD Flue gas Desulphurisation
CFBC Circulating Fluidised Bed Combustion
PFBC Pressurised Fluidised Bed Combustion
IGCC Integrated Gasification Combined Cycle
NGCC Natural Gas Combined Cycle

2.1.2 CO_2 capture technologies

To capture CO_2 from power plants and industrial processes, three techniques can be applied. In the first (end-of-pipe approach) CO_2 is recovered from the flue gas by scrubbing with an aqueous solution, e.g. amines. The post combustion capture using amine scrubbing is the technology closest to implementation, while novel concepts are developed at the same time, such as molecular scale absorbents. In the second approach the fossil fuel is converted into hydrogen through reforming and water gas shift reaction, and CO_2 is recovered from the product stream (pre-combustion). Research and development focuses on membrane technologies, high temperature membranes for H_2 separation, membranes tolerant to sulphur, membrane reforming, as well as on gasification and gas cleanup. In the last approach O_2 is used instead of air in the burner (oxy-fuel combustion), and requires air separation upstream the combustion.

There are few full-scale oxy-fuel combustion plants in operation; so far, mainly laboratory work, pilot plants and studies have provided understanding of the relevant design parameters and operational issues. In addition, priority is put on retrofitting existing boilers, therefore, considerable research and design efforts focus on matching air and oxygen combustion in terms of heat transfer, flame temperatures and flows. There have been some pilot plant applications in the United States (Air Liquide), Canada (CANMET), Europe (International Flame Research Foundation – IFRF, Alstom/Vattenfall, CIUDEN), and Japan (Ishikawajima-Harima Heavy Industries - IHI), applying the oxy fuel technology. Studies have also assessed the feasibility and economics of retrofits and new power plants. Several recent assessments have compared oxy-fuel technology with post-combustion capture and IGCC technologies for CO_2 abatement cost. These studies indicate that oxyfuel combustion is a favourable option but the comparison depends on the plant considered and the associated emission abatement technologies employed, which are determined by the regulation regimes of different countries.

2.2 Oxy-fuel combustion systems

2.2.1 Description of concept

There are two types of oxy-fuel systems: oxy-fuel boilers (either a retrofit or new design) and advanced oxy-fuel combustion systems e.g. advanced gas turbine systems. The former are close to demonstration at a commercial scale, while the latter (such as chemical looping combustion systems and novel power cycles using CO_2/water as working fluid) are still at the design stage. The current review focuses on evaluating and presenting the possibility of combining oxyfuel combustion boilers with mild combustion techniques applied to solid fuels including mixtures of coals/biomass, therefore no reference will be made to oxy fuel advanced gas turbine cycles, chemical looping systems or advanced ceramic membrane systems.

The oxy-fuel combustion process eliminates nitrogen from the flue gas by combusting a hydrocarbon fuel in either pure oxygen or a mixture of pure oxygen and a CO_2 - rich recycled flue gas (carbonaceous fuels include biomass). Combustion of fuels with pure oxygen reaches adiabatic combustion temperatures around 3500°C which is far too high for typical power plant materials. The combustion temperature is controlled by the proportion of flue gas and gaseous or liquid-water recycled back to the combustion chamber. The combustion products consist mainly of carbon dioxide and water vapour together with excess oxygen required to ensure complete combustion of the fuel. It will also contain any other components, possibly inert gaseous compounds like Ar and traces of N_2, diluents in the oxygen stream supplied and from the atmospheric air leakage into the system. After cooling to condense water vapour, flue gas contains about 80-98% CO_2 depending on the particular oxy-fuel combustion process. This concentrated CO_2 stream can be compressed and further purified before delivery into a pipeline for storage. The CO_2 capture efficiency is very close to 100% in oxy-fuel combustion capture systems. Impurities in the CO_2 are gas components such as SO_x, NO_x, HCl and Hg derived from the fuel used, and the inert gas components, such as nitrogen, argon and oxygen, derived from the oxygen feed or air leakage into the system. Inert gases must be reduced to a low concentration to avoid two phase flow conditions developing in the pipeline systems. The acid gas components may need to be removed to comply with legislation covering co-disposal of toxic or hazardous waste or to avoid operational and environmental problems due to disposal in deep saline reservoirs, hydrocarbon formations or in the ocean. The carbon dioxide stream must be dried to prevent water condensation and corrosion in pipelines and to allow use of conventional carbon-steel materials.

Although elements of oxy-fuel combustion technologies are in use in the aluminium, iron and steel and glass melting industries today, oxy-fuel technologies for CO_2 capture have yet to be deployed on a commercial scale. A general process flow sheet is provided in Figure 2.1.

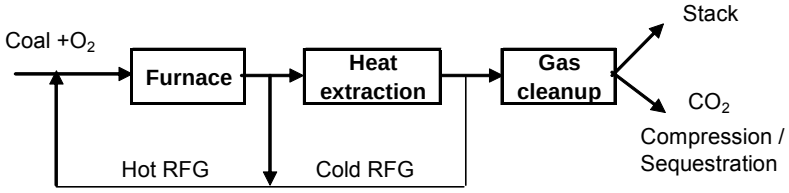

Figure 2.1 *General flow sheet for oxy-fuel combustion [3]*

The characteristics of oxy-fuel combustion with recycled flue gas differ with air combustion in several aspects including the following [4]:

- To attain a similar adiabatic flame temperature the O_2 proportion of the gases flowing through the burner is typically 30%, while in air combustion it is ~ 21%, and about 60% of the flue gas is recycled.
- The high proportions of CO_2 and H_2O in the flue gas result in higher gas emissivity, so that different radiative heat transfer for a boiler retrofitted to oxy-fuel will be attained when the O_2 proportion of the gases flowing through the burner is kept constant.
- The volume of gas flowing through the furnace is reduced somewhat, and the volume of flue gas (after recycling) is reduced by about 80%.
- The density of the flue gas is increased, as the molecular weight of CO_2 is 44, compared to 28 for N_2.
- Without gas cleaning in the recycle stream, emissions including corrosive sulphur gases show higher concentrations than in air firing.
- As oxy-fuel combustion combined with sequestration must provide power to several significant unit operations, such as flue gas compression, that are not required in a conventional plant without sequestration, oxy-fuel combustion / sequestration is less efficient per unit of energy produced. However, it is more efficient than a conventional plant with sequestration due to the significant energy required scrubbing a dilute gas stream prior to compression.

Coal-fired oxy-fuel combustion has been evaluated for a number of purposes for some years. Already in 1972, use of pressurised CO_2 was proposed for Enhanced Oil Recovery [2], [6]. The gas that dissolves in the oil to lower its viscosity and improve its flow rate expands in the reservoir to push additional oil to a production well bore. Gas injection accounts for nearly 50 percent of EOR production in the United States [7]. In metal heating furnaces, recycling of hot recycled flue gas (RFG) was suggested to reduce furnace size and NO_x emissions.

The oxygen production technology is a key parameter in the oxy-fuel capture systems. Current methods of oxygen production by air separation comprise cryogenic distillation, adsorption using multi-bed pressure swing units and polymeric membranes.

2.2.2 Current state of the art on oxyfuel combustion of solid fuels

Experimental studies on oxy-fuel combustion: Status of research

A number of studies on oxy-fired pulverised coal power plants have investigated the characteristics of pulverised coal oxygen combustion. An effort was made to summarise the focus and the main findings of these works. In short, research focused on:

- Calculation of the flame propagation velocity and flame stability, adiabatic temperature and flame temperature using simulation codes.
- Heat transfer calculations (combustor design), thermal radiation with the enrichment of O_2 in the oxidizer.
- Pure O_2 injection at the centre of the burner to study the effect on the ignition and flame stability in the furnace, NO_x emissions, unburnt carbon content of the ash
- NO_x conversion comparison between oxygen and air combustion, studies on NO_x reduction mechanisms in oxy-fuel combustion (N conversion to HCN and NH_3 in the flame, gas staging)
- Gas cleaning prior to recycling flue gas to the combustor, mainly due to SO_x concentrations, study of desulphurisation efficiency in relation to SO_2 residence time and SO_2 enrichment in the furnace, $CaSO_4$ decomposition in relation to high SO_2 concentrations
- Soot formation and soot particles agglomeration upon increase in the oxygen content of the oxidizer
- Fuel and oxygen velocities on the flame length and soot formation (turbulent mixing and entrainment phenomena)
- Improvement and modification of models and correlations for oxy-fuel flames

Table 2.2 shows an overview of the laboratory studies conducted on oxyfuel combustion as reported in [4].

Assessments of pilot and full scale oxy-fuel combustion plants: Overall plant performance (retrofit and new plant)

Tables 2.3 and 2.4 list some of the pilot studies and full scale facilities for oxy-fuel combustion reported in literature [4], [30].
The earliest study of coal oxy-fuel combustion in a pilot-scale furnace was carried out for the Argonne National Laboratory (ANL) by the Energy and Environmental Research Corporation (EERC) in their 3 MW_e pilot facility [31]. The objective of the study was to characterise the operational issues and to provide a basis for scaling up. Lower NO_x and SO_x emissions were measured while no operational difficulties were found for oxy-fuel combustion. An extensive study carried out by the International Flame Research Foundation (IFRF) evaluated the combustion of pulverised coal in a mixture of O_2 and recycled flue gas with the primary consideration of retrofitting an existing PF boiler [32]. The following conclusions were drawn:
- Oxy-fuel combustion is technically feasible in a single wall-fired burner management.
- The optimised oxy-fuel combustion flame yielded similar radiative and convective heat transfer performance to normal air operation, and also yielded in-flame gas composition trends, combustion performance, flame length and flame stability comparable to normal air combustion by tuning the recycled flue gas ratio to the coal type and the combustion facility.
- Oxy-fuel combustion is able to achieve the combustion performance (e.g. combustion efficiency and pollution emissions) similar to air operation, and was therefore applicable for PF boiler retrofitting. The maximum flue gas CO_2 concentration is 91.4% or even higher under fully optimised conditions.
- Oxy-fuel combustion significantly decreases NO_2 emissions (mg/MJ coal). Low NO_x burner technology was also demonstrated to be viable using oxy-fuel combustion technology.

The effects of several factors on oxyfuel combustion performance include oxygen concentration or recycled ratio, O_2 purity, wet/dry recirculation, and burner performance were studied and the following conclusions were drawn ([35], [38], [39], [4]):

- CO_2 concentration in the flue gas achieved close to the theoretical value (average 92%)
- Increasing the inlet oxygen concentration increases the flame temperature. The oxygen purity (less than 5% N_2 in the O_2/ CO_2 mixture) has no significant effect on the flame temperature.
- NO_x emissions (mass per unit of energy released from the coal) decreases compared to that in air combustion. The reduction was shown to depend on the oxygen concentration due to the change in the flame temperature. However, the difference decreases significantly even if as little as 3% N_2 presented.
- SO_2 emission (mass per unit of energy released from the coal) was not affected significantly by the variations of O_2 or CO_2 concentration. The decrease in SO_2 during oxy-fuel combustion is due to SO_3 formation and subsequent sulphur retention.
- CO concentration is not a considerable problem. Increasing the oxygen concentration decreased the CO emission. The decrease of CO concentration along the flame is slower compared to air combustion because of high CO_2 gas concentration in oxyfuel combustion.
- The experimental results compared well with the modelling efforts, indicating that CFD code could be used for exploring oxy-fuel concepts.

It should be noted that even when recycling 2/3 of flue gas to maintain a 35% by volume O_2 feed to a pulverized coal fired boiler, hot recycling of the flue gas prior to CO_2 purification and compression still reduces the size of all unit operations in the stream leaving the boiler compared to that of similar equipment deployed in conventional air blown combustion systems. The overall reduction in flow volumes, equipment scale and simplification of gas purification steps will thus have the benefit of reducing both capital and operating costs of equipment deployed for combustion, heat transfer and final gas purification in process and power plant applications [4].

A comprehensive review of studies on oxyfuel combustion is given in [40]. In most of these studies, 90% or more of the CO_2 is captured producing a 98% pure CO_2 stream. For retrofitting an existing sub critical steam PC plant, the data show the importance of the base plant efficiency. It is argued that only high efficiency modern power plants should be considered for retrofitting, given the large efficiency penalty imposed, mainly due to the air separation unit that takes about 20%, and the CO_2 purification, compression-liquefaction, consuming 12–14% of the gross electricity output of the plant, representing about 1/3 of the plant's output. The net plant efficiency with CO_2 capture is between 23% and 26% (LHV). For retrofitting a higher efficiency supercritical PC plant, the energy penalty of CO_2 capture is much lower: the total energy output of the plant is reduced by about 20% and conditions are even more favorable for new supercritical PCs plant with a net efficiency of about 34% (LHV).

The IEA Greenhouse Gas R&D Program (IEA GHG) has assessed the performance and costs of new power plants with and without CO_2 capture [41]. Studies were carried out for IEA GHG by the following leading engineering contractors and process developers:
- Post combustion capture: Fluor, in collaboration with Mitsui Babcock and Alstom, and MHI.
- Pre-combustion capture (IGCC): Foster Wheeler, with data from gasification and gas treating vendors.
- Oxy-combustion: Mitsui Babcock, in collaboration with Air Products and Alstom.

The optimum power generation and CO_2 capture technologies will depend on various criteria which will depend on local circumstances and utilities' preferences. Further work is needed to assess power generation with CO_2 capture at a range of different locations

worldwide and to assess the abilities of capture processes to accommodate the present and future operational requirements of power utilities.

Several studies demonstrated the oxy-fuel technology either wit sub critical supercritical steam cycle power plants [2], [42], [43], [44], [45]. The overall thermal efficiency on a lower heating value basis is reduced, in the range of ~45% to 35 %. Some of the conclusions of the system studies include:

- The CO_2 -rich flue gas from the boiler to be recycled back to the combustor is cooled by direct water scrubbing to remove residual particulates, water vapour and soluble acid gases such as SO_3 and HCl.
- A low temperature (-55°C) CO_2 purification plant integrated with the CO_2 compressor could not only remove excess O_2, N_2, argon but can also remove all NO_x and SO_2 from the CO_2 stream, if high purity CO_2 is required for storage. Significantly, removal of these components before final CO_2 compression eliminates the need to otherwise incorporate upstream NO_x and SO_x removal equipment in the net flue gas stream leaving the boiler. Elimination of N_2 from the flue gas results in higher SO_x concentrations in the boiler and reduced NO_x levels. Suitable corrosion resistant materials of construction must be chosen.
- The overall heat transfer is improved in oxy-fuel firing because of the higher emissivity of the CO_2 /H_2O gas mixture in the boiler compared to nitrogen and the improved heat transfer in the convection section. These improvements, together with the recycle of hot flue gas, increase the boiler efficiency and steam generation by about 5%.

The overall thermal efficiency can be improved by operating the O_2 plant air compressor and the first and final stages of the CO_2 compressor without cooling, and recovering the compression heat for boiler feed water heating prior to de-aeration

Table 2.2 *Summary of laboratory studies cited in [4]*

Focus of Study	Research conditions	Location
Ignition characteristics and flame propagation speed.	Flame propagation in coal-dust clouds in a microgravity facility; Experiments were carried out in O_2/CO_2, O_2/N_2 and O_2/Ar atmospheres at O_2 concentrations ranging ~ 20 - 95%	[8]
Char combustion reactivity and effect of CO_2 presence.	Atmospheric and a pressurised thermogravimetric analyses were done using varying heating rate and O_2 (0–100%) concentrations in mixtures of O_2/CO_2 and O_2/Ar	[9], [10]
Char combustion reactivity at temperatures prevailing in practice.	Pulverised coal particles were burned in an entrained-flow reactor, at a gas temperature of 1700K and over oxygen concentrations in N_2 ranging from 6 to 36%.	[4]
NO_x reduction mechanisms in coal combustion with recycled CO_2	Pulverised coal particles were burned in a flat CH_4 flame (entrained-flow reactor) at an oxygen concentration of 21% with varied CO_2 concentration in Ar and at a flame temperature of 1450^oC	[11]
Reduction of recycled NO_x at low recycling ratio, effects of fuel equivalent & recycling ratio, coal properties.	Pulverised coal particles combust in an entrained-flow reactor at a recycling ratio of 0–0.4 and a temperature of 1123–1573 K.	[12], [13], [14]
Sulphation of limestone and influences of various factors on SO_x formation.	Desulphurization reaction was performed on a fixed bed reactor with a model flue gas (10% O_2 and 80% CO_2) at temperatures of 1013–1363 K; $CaSO_4$ decomposition was studied in an entrained-flow reactor with model flue gas (O_2: 0–30%, CO_2: 0–100%) at a temperature of 1400–1600 K); modelling approach was also used.	[15], [16]
CO/CO_2 ratio inside char particles.	A detailed char particle combustion model was used to calculate the CO/CO_2 in char particle and to simulate influence of the variation of CO_2 and O_2 in the bulk gas.	[17]
Environmental assessment of coal combustion in O_2/CO_2 mixture compared with that in air.	Equilibrium calculation was carried out with FACT to assess the emissions of SO_x, NO_x, CO and trace elements, and the ash composition of coal combustion in O_2/CO_2 compared to those in air.	[18]
Heat transfer assessment of retrofit .	The convective and radiative heat transfer in an existing boiler was modelled using HYSYS to determine the impact of retrofit to oxy-fuel combustion.	[4]
Heat transfer assessment of retrofit .	CFD code combined with a band model to estimate gas emissivity was used to assess the possibility of retrofitting an air-fired boiler for oxy-fuel combustion.	[4]
Experimental investigation of the flame structure and emission characteristics of a 30 kW oxy-fuel combustor. Influence of fuel and oxidizer velocity, with or without a quarl, on NO emissions.	Elevating the nitrogen-in-oxidizer percentage up to nearly 20%. Fuel or oxidizer velocity parameter (because of the different turbulent intensity, entrainment of the recirculated product gas to flame zone.). Effect of a swirler or quarl on flame stabilization and NO emissions (due to burning velocity).	[19]
Development of an experimentally validated mathematical model of soot formation in oxygen-enhanced flames.	The soot volume fraction was measured as a function of oxygen content in the oxidizer jet at different strain rates from 10 to 60 s^{-1} and at constant oxygen content on the oxidizer side.	[20]
Combustion characteristics, flame structure and length in oxyfuel burner.	Testing of various fuel nozzle diameters and fuel / oxidizer velocities, to vary the inlet flow velocities. The overall equivalence ratio is 0.98. Flame length measured by varying fuel / oxygen velocities.	[21]
Quantitative, spatially resolved, laser-saturated fluorescence measurements of nitric oxide concentration in sooting, high-temperature, oxygen-methane, counter-flow diffusion flames.	Six different flames containing 1%, 3%, and 10% N_2 in either the oxidizer or fuel streams are investigated at a global strain rate of 20 s^{-1}. Excitation of NO is obtained at 224.45 nm in the γ(0,0) band and detection is performed in a 2-nm region centered at 235.78 nm in the γ(0,1) band. Numerical computations for all counter-flow diffusion flames are conducted using OPPDIF with GRI Mech-3.0. The effect of gas-phase radiation is considered in the modeling.	[22]

Focus of Study	Research conditions	Location
Simultaneous CO_2 recovery and reduction of SO_x and NO_x in O_2/CO_2 coal combustion with heat recirculation.	Experimental investigation of the kinetics of desulphurisation and $CaSO_4$ decomposition in atmospheres of high CO_2 and SO_2 concentrations in a fixed bed and an entrained flow reactor. Concentrations of O_2 and CO_2 were 10% and 80% respectively.	[23]
NO_x emissions reduction at high temperatures using staged combustion or flameless oxidation.	Tests in a furnace with indirect cooling and controlled temperature at 1200 - 1600^oC. Effect of combustion air temperature, fuel/air ratio, burner turn down ratio, furnace chamber temperature, staged combustion, oxygen concentration and flue gas recirculation on NO_x emissions.	[24]
Laboratory study on the combustion emissions from pulverized solid fuels: NO, (NO and NO_2), SO_x, CO and CO_2.	Coal, waste tire crumb and waste plastics were burned in an electrically heated drop-tube furnace at high particle heating rates (10^4- 10^5 K s^{-1}) and elevated gas temperatures 1200 - 1600^oC. The fuel to air bulk equivalence ratio, φ, was varied between 0.4-l .8. A mixture of O_2 / CO_2 /Ar was used as oxidizing gas.	[25]
Emission characteristics of CO_2, SO_2 and NO_x in the flue gas of coal combustion.	Varying the compositions and concentrations of feed gas ($O_2/CO_2/N_2$) and the ratios of recycled flue gas. The differences between O_2/recycled flue gas combustion and general air combustion are discussed.	[26]
Measurement of the combustion rates of two pulverized coal chars in both conventional and oxygen-enriched atmospheres.	A combustion-driven entrained flow reactor equipped with an optical particle-sizing pyrometry diagnostic and a rapid-quench sampling probe has been used for this investigation. High value sub bituminous coal and a high-volatile bituminous coal have been investigated, oxygen concentrations ranging from 6 to 36 mol% and gas temperatures of 1320–1800 K.	[27]
Fuel conversion from oxy-fuel combustion in a circulating fluidized bed.	Brown coal behaviour in increased oxygen concentration, varying temperatures and fuel loads in a laboratory-scale CFB combustor. Oxygen concentration in the oxidiser stream (mixtures of O_2+N_2 and O_2+CO_2): 21-60%; combustor's temperature: 973-1133 K. Carbon, sulphur and nitrogen conversion ratios were calculated.	[28]
Pulverized coal combustion in air and in O_2/CO_2 mixtures with NO_x recycle.	20 kW vertical pf-burner combustor, O_2/CO_2 mixtures with NO_x recycle. Effect of combustion media, combustion mode (staging or non-staging) and recycling location on NO_x emissions.	[29]

Table 2.3 *Summary of pilot-scale studies cited in [4], [30]*

Organisation	Furnace used	Focus of study	Cited
EERC and ANL, USA	3MWth utility boiler pilot facility	Demonstrating the technical feasibility of the CO_2 recycle boiler. Determining the ratio of recycle gas to O_2 for achieving heat transfer performance similar to air firing. Quantifying the observable operational changes such as flame stability, pollution emissions, burnout. Providing a basis for scaling experimental results to commercial scale.	[31,5]
IFRF, Netherlands	IFRF furnace 1: 2.5 MW, the furnace with internal square cross-section of 2x2 m and 6.25 m long and an air-staged swirl burner	Evaluating the combustion of pulverised coal during oxy-fuel combustion for retrofitting existing pulverised coal fired boilers to maximise the CO_2 concentration in flue gas. Optimising oxy-fuel combustion conditions to yield similar radiative and convective heat transfer performance to air firing. Evaluating the impact of oxy-fuel combustion on furnace performance, including flame ignition and stability, heat transfer, combustion efficiency, pollutant emissions, compared to air operation.	[32]
Doosan Babcock, UK	Multi-Fuel Burner Test Facility (MBTF) - Preconversion	Oxyfuel firing vs. Air firing, Two coals, Investigate effect of: Burner stoichiometry, Flue gas recycle ratio, Transport CO2 oxygen content. Parameters measured: Process conditions, Flue gas analyses, Carbon in ash.	
IHI, Japan	IHI's 1.2 MW combustion-test furnace: horizontal cylinder furnace with 1.3 m inner diam.. 7.5 m length and a swirl burner	Combustion characteristics of pulverised during oxy-fuel combustion.	[4,33] [34]
Air liquide, B&W, USA	1.5 MW pilot-scale boiler with air staged combustion system	Demonstrating the technical feasibility retrofitting air to oxy-fuel combustion for large scale boiler. Highlighting the impacts of oxy-fuel combustion process on pollutant (NO_x, SO_2 and Hg) emissions and boiler efficiency	[4]
CANMET, Canada	Vertical combustor research facility (300 kW): cylindrical, down-fired, adiabatic vertical combustor, inner diameter 0.60m & length 6.7 m.	Pulverised coal combustion behaviours in various O_2/RFG mixtures, compared with air combustion. Demonstrating the technical factors on the combustion performance.	[4,35] [36]

Table 2.4 *Summary of Large Scale Pilot and Demonstration Oxyfuel Projects [4] [37]*

Project	Location	MWth	Start Up	Boiler Type	Main Fuel	CO_2 Train
B&W	USA	30	2007	Pilot PC	Bituminous, Sub-Bituminous, Lignite	No
Jupiter	USA	20	2007	Industrial No FGR	NG, Illinois No. 6 Coal	No
Vattenfall (Schwarze Pumpe)	Germany	30	2008	Pilot PC	Lignite (Bituminous)	With CCS
Alstom (Windsor Facility)	USA	15	2009	Pilot PC (Tangential)	Bituminous, Sub-Bituminous, PRB	No
Oxy-coal UK	UK	40	2009	Pilot PC	Bituminous	No
Total/Lacq	France	30	2009	Industrial	NG	With CCS
Pearl Plant	USA	66	2009	22 MWe PC	Bituminous	With CCS (Side Stream)
Callide	Australia	90	2010	30 MWe PC	Bituminous	With CCS
Ciuden -PC	Spain	20	2010	Pilot PC	Anthracite, Bituminous, Lignite, Petroleum Coke	Unknown
Ciuden – CFB	Spain	30	2010	Pilot CFB	Anthracite, Bituminous, Lignite, Petroleum Coke	Not known
Praxair (Jamestown)	USA	150	2013	50 MWe CFB	Bituminous	With CCS
Endessa/Ciuden	Spain	~1500	2015	300 MWe CFB (?)	Unknown	With CCS
Vattenfall (Janschwalde)	Germany	~1000	2015	~250 MWe PC	Lignite (Bituminous)	With CCS
Black Hills Power/B&W	USA	~ 400	2015	~ 100 MWe PC	Bituminous, PRB	Not known
KOSEP/KERPRI ((Youngdong)	S. Korea	~400	2018	~100 MWe PC	Not known	Not known

Focus of research and technological development

One of the promising technologies for carbon capture and sequestration in coal utilisation for power generation industry is by ultra-supercritical boilers using oxygen combustion and recycle flue gas. The following Table 2.5 lists the advantages and disadvantages of oxy fuel combustion, as presented in [4], according to the present state of the art and taking into account the on going research in the field.

Table 2.5 *List of the advantages and disadvantages of oxy-fuel combustion [4]*

Advantages	Disadvantages
Industry familiar with oxyfuel technology (glass, steel & iron, cement) and potentially represents a lower commercial and technical risk than for CO_2 capture with e.g. coal gasification technology. Suitable for near-zero emissions. Potential to be retrofitted to existing plant Can be implemented in new plants as stand by equipment Low NO_x emissions relative to conventional PF technology	Reduced efficiency compared to currently used PF technology (Air separation Unit). Not demonstrated extensively. Lack of attractive funding and subsidy schemes Oxy-fuel based near-zero electricity economy not compatible to the 'hydrogen economy'. Negative public perception on CCS in general, as opposing the renewable energy growth, storage of CO_2

The main technical issues are summarised in Table 2.6.

Table 2.6 *Overview of Overall Oxyfuel technology issues [as given by RWEn, UK]*

Safety issues	Furnace and burner related issues	Operational issues	Studies
Safety handling and storage of CO_2 & O_2	Selection of coals, use of biomass	Air leakage	Regulation issues
Flame detection issues (higher CO_2 and moisture may affect UN and IR absorption)	Carbon burnout	Optimum RR, Gas recirculation	CO_2 purity limits for oxyfuel
Safety of mixing O_2/CO_2	Slagging, corrosion, fouling	Air heater design	Pre investment issues compared with post combustion capture
Flame stability	NO_x chemistry needs to be understood	Optimisation of mixing strategy (where to add O_2)	Required footprint for retrofit (e.g. air separation unit)
Safe switch over to oxyfuel combustion	Heavy metal recycling and ash composition	Oil burner operation on oxyfuel	
Safety of staff with CO_2/flue gas leaks	Burnet design	Flexibility – start up/shutdown limited by air separation unit so cold start on air	
Purging for safety	Heat transfer		

In more detail, the critical technological issues for meeting the challenge of CO_2 emission reduction using oxyfuel technology are:

- Development of ion transport membranes, other novel oxygen production systems to replace ASUs (oxyfuel combustion)
- Large-scale transport of CO_2, captured and pressurized at coal combustion and conversion plants, to injection at storage sites.
- Technologies that tolerate variable coal qualities, e.g. high-slagging coal
- General burner improvements for oxyfuel application (flame characteristics, heat transfer)
- Establish gas cleaning requirements prior and after recirculation
- Low cost mercury and other trace metals removal and measurement systems
- Develop computational fluid dynamics (CFD) modeling capability to complement the pilot-scale experimental investigations.
- Experimental data for oxy-fuel combustion are quite limited. Thus, the design of oxy-fuel combustors requires more comprehensive research efforts, including a sequence of trial and error testing, combustion measurements, and analysis.

Experimental study of oxygen pulverised fuel combustion should include a wide range of operational parameters and various fuel qualities. More specific, lab scale tests should focus on:

- Effect of recirculation on emissions concentration in the furnace, especially NO_x and SO_x. Study of fuel – N fate during oxygen combustion.
- Study of devolatilisation and char combustion rates with respect to recirculation ratio and fuel characteristics.
- Optimum position of O_2 injection with respect to flame stability, char burn out, flame velocity, flame temperature, NO_x formation.

- Varying coal and biomass qualities (high ash, variableN/S content); tests with pre treated biomass and coal.
- Deposition studies on heat transfer surfaces with respect to varying solid fuels properties, such as ash quantity and composition, with varying oxygen concentration recirculation rates and flame temperature.

2.3 Literature review on coal/biomass co firing under oxyfuel conditions

An overview of research activities and technology developments on oxy-fuel combustion including char combustion temperatures, fuel burnout, gas composition, heat transfer, coal reactivity and flame ignition has been recently published by Wall et al. [46]. The characteristics of combustion under O_2/CO_2 differ from air combustion in several aspects, e.g. gas composition, gas density, flow field. This different gas environment experienced by fuel particles might have an impact on the combustion processes including ignition, combustion characteristics, char reaction, and subsequently, ash and pollutants formation [47]. The consequence of this becomes important when the pulverized fuel boilers are planned to be retrofitted to oxyfuel. The effect of oxyfuel combustion on trace elements emissions and fly ash size distribution is uncertain, but it is expected that the behaviour of minerals will be affected by the change in environment. For example, the high carbon dioxide partial pressures under oxyfuel will increase the decomposition temperature of carbonates [48]. Therefore in this introductory section an effort is made to gather the relevant literature on the parameters that are expected to affect the inorganic elements vaporization and ash deposition behaviour in the combustor.

Ash particle formation under oxy-fuel combustion has been addressed by Sheng et al. [47, 49, 50]. Specifically in [47] coal ash particles were collected at the bottom of a drop tube combustor using a low pressure impactor. It was found that O_2/CO_2 combustion shifted the size of the submicron mode center to smaller size and decreased the yield of the submicron particles as compared to air combustion, for the same oxygen concentrations, while increasing the oxygen concentration decreased the difference between the two combustion atmospheres. In [50], pulverized coals were fired in O_2/CO_2 and O_2/N_2 mixtures in a drop tube furnace. Qualitative XRD analysis showed that, in comparison to O_2/N_2 combustion, O_2/CO_2 combustion did not significantly change the main crystalline phases formed in residue ashes, implying no significant impacts on ash formation behaviors of the main coal minerals. Mössbauer spectroscopic analysis indicated that the variation between O_2/CO_2 and O_2/N_2 combustion did not affect the ash formation mechanisms of iron-bearing minerals, but affected the relative percentages of iron species formed in the ashes. O_2/CO_2 combustion resulted in more iron melting into glass silicates in the ash. The differences observed in the ash formed under the two atmospheres were attributed to the impact of combustion gas atmosphere on coal char combustion temperatures, which influenced the ash formation behaviors of included minerals.

The experimental work of Suriyawong et al. [51] focused on ash formation under O_2/CO_2 combustion of a sub bituminous coal in a drop tube furnace; it was observed that the mean size of submicron ash particles formed in O_2/CO_2 combustion was smaller than that formed in conventional air combustion. In [46] on the contrary, the size distribution and chemical composition of bulk fly ash did not differ significantly when produced in oxy-fuel combustion and air combustion. The work described in [52], burning a high-aluminium coal in a drop tube furnace to compare the ash formation in O_2/CO_2 combustion and air combustion, shows that O_2/CO_2 combustion did not significantly affect the transformations of main minerals, but did affect the fine ash formation, consistent with the observations of Suriyawong et al. [51].

A significant proportion of the submicron ash generated during coal combustion is believed to be the result of mechanisms including the vaporization and homogeneous condensation processes of refractory oxides such as SiO_2, CaO, MgO and Fe_2O_3 [50], [52], [53]. A number of studies focus on solid fuel/char burnout in O_2/CO_2 environments. Bejarano and Levendis [54] conducted a fundamental investigation on the combustion of single particles of coal in O_2/N_2 and O_2/CO_2 environments. They observed increasing particle temperatures and decreasing burnout times for increasing oxygen fractions, being the particle temperature higher and the burnout time lower for the O_2/N_2 environment at the same oxygen molar fraction. They reported equivalent bituminous coal volatile and char temperatures to those measured in air when the oxygen content in the O_2/CO_2 mixture was ~30%, whereas this concentration had to be 30-35% to attain similar burnout times. In [55] the combustion rates of two pulverized coal chars were measured in both conventional and oxygen-enriched atmospheres. Predicted char particle temperatures tended to be low for combustion in oxygen-depleted environments. In [49] the impact on mineral transformation and fine ash formation of O_2/CO_2 combustion of a high-aluminum ash coal was studied. The main conclusion here as well was that O_2/CO_2 combustion had an impact on the local char particle combustion temperature and consequently on the ash vaporization and the ash mineral composition. The varying bulk gas composition (e.g., CO_2 concentration) changed the O_2/CO_2 ratio within the burning char particle affecting the vaporization of refractory oxides, as observed by Krishnamoorthy and Veranth [56], who modelled the combustion of a single char particle. As a consequence, this affects accordingly the chemical composition of fine ash particles. The varying char combustion temperatures and locally reducing conditions might reduce minerals to more volatile forms. Char temperature fluctuations between air and oxyfuel combustion, affect therefore the degree of release of the included minerals and alter their extent of vaporization. Reducing conditions may also have a notable impact on excluded minerals, particularly iron-based minerals [57].

Zheng and Furimsky [58] carried out chemical equilibrium calculations using the software FACTSage® to study the effect of CO_2 on the emissions and the ash composition under coal combustion. They concluded that the combustion medium had little effect on the ash chemical composition, but they did not exclude the effect of the carbonation and/or sulfation reactions of basic components on ash composition for the coals containing a high alkaline mineral matter. However it was not stated if molten ash phases are included as possible products in the calculations. Zhao et al. [59] applied the same approach to study the evaporation of mineral elements in O_2/CO_2 combustion. For temperatures lower than 2000K they did not find differences between the combustion in air and O_2/CO_2 .
Although significant work exists studying the interactions of S/K/Cl and their significance in fine ash and aerosol formation, explaining in detail the possible mechanisms that lead to the main ash elemental composition of fine ash and aerosols, e.g. [60, 61], so far little work is reported on the possible effect of oxyfuel combustion conditions on the elemental composition as well as the fine ash yield in comparison to conventional air firing.

Considering biomass co fired with coal under oxyfuel conditions, there is only one published work to our knowledge. Tests in an entrained flow reactor to study the ignition and burnout of coals and blends with biomass under oxy-fuel and air (reference) conditions by Arias et al. [62], showed worsening of the ignition temperature in O_2/CO_2 mixtures when the oxygen concentration was the same as that of the air; however at oxygen concentrations of 30% or higher, an improvement in ignition was observed. The results of this work indicate that coal burnout can be improved by blending biomass in O_2/CO_2 mixtures.

3. Description of experimental facility and test procedure

The most prominent example of a lab-scale installation for dynamic fuel characterisation is a so-called Drop Tube Furnace. In its basic form, the installation constitutes of a vertical reactor, which is externally heated, mostly by an electric furnace. The Lab-scale Combustion Simulator, developed and optimised in the past decade by ECN is a good example of such advanced DTF. The ECN lab-scale combustion simulator (LCS) shown in Fig. 3.1, consists of an extensively modified drop-tube furnace, equipped with a flat-flame, multi-stage, premixed gas burner, into which the investigated solid pulverised fuel is injected. This provides adequate heating rates (10^5 K/s), well in range with full-scale PC boilers. The reactor is equipped with a conical inlet, which causes the flue gas and char/ash particles to decelerate, enabling for long residence times in spite of a relative short length. The char particles are then lead into an electrically-heated reactor tube, where they are further combusted. The staged gas burner accommodates high initial heating rates and temperatures and provides the possibility to simulate air staging as in low-NO_x burners and also the presence of specific combustion products such as, e.g., SO_2. The furnace has ~1 m length. The burner consists of two concentric sub-burners viz. a primary, inner burner (10.9 mm ID) and a secondary, outer burner (60.7 mm ID). The inner burner is supplied with a mixture of O_2, CH_4, and CO_2 or N_2 with an oxygen-lean rate. In the outer burner the gaseous mixture of O_2, CH_4, and CO_2 or N_2 provides the necessary oxygen in order to complete the combustion. Fuel particles are fed through the inner burner and are rapidly heated (>10^5 °C/s) to the high temperature level of, e.g., a coal flame (1400-1600 °C). Typically, low particle feed rates of 1-5 g/h are used in order to control the gaseous environment of each particle by means of the imposed gas burner conditions. This implies that heating and devolatilisation of the fuel particles takes place in an oxygen-deficient zone (indicated as I in Figure 3.1) provided by the primary, inner burner, whereas subsequent char combustion takes place in a zone with excess oxygen (indicated as II in Figure 3.1). The transition from oxygen-lean to oxygen-rich takes place and is completed in zone I by diffusion. The resulting gas/particle flow is then drawn into a 76 mm internal diameter alumina reactor tube for complete oxidation of the fuel. From a distance of ~130 mm from the burner the tube is surrounded by two 3.4 kW furnace sections equipped with Kanthal Super 1800 elements with a maximum element temperature of 1700°C. The temperature of each zone is independently controlled by a Eurotherm controller and two S-type thermocouples, at 1450°C. The furnace temperature profile (Fig. 3.2 a & b) was measured in the absence of the particles, using S-type thermocouples of 0.05 mm diameter. The left T-profile is the very first one at the start of the oxyfuel work while the right profile is the more recent one, based on which the conclusions are finally drawn. The profile was measured several times, in order to improve and achieve absolutely comparable and homogeneous profiles. The first and last measurements are presented in Figure 3.2. During the tests, the second profile was applied. The flue gas composition was continuously monitored using a UltraViolet analyzer for NO and NO_2, a NDIR for CO and CO_2 and a magneto mechanical analyzer for O_2.

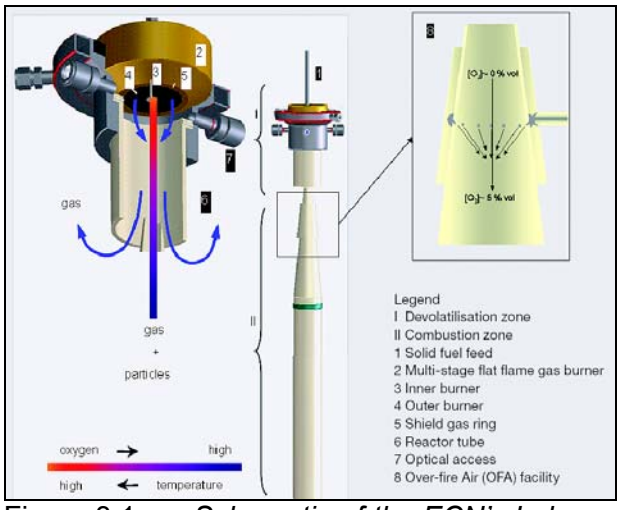

Figure 3.1 *Schematic of the ECN's Lab-scale Combustion Simulator (LCS. Legend: I Devolatilisation zone, II Combustion zone, 1 Solid fuel feed, 2 Multi-stage flat flame gas burner, 3 Inner burner, 4 Outer burner, 5 Shield gas ring, 6 Reactor tube, 7 Optical access*

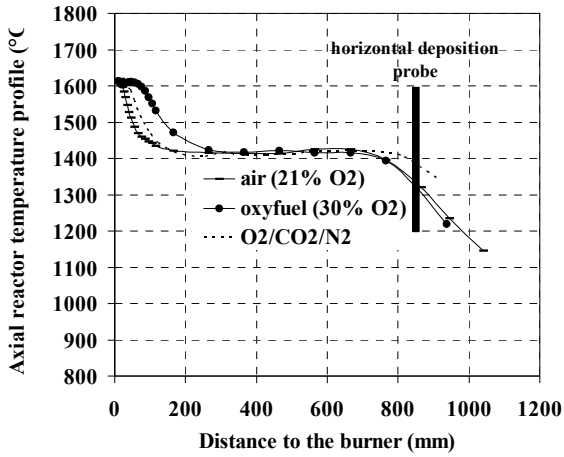

(a)

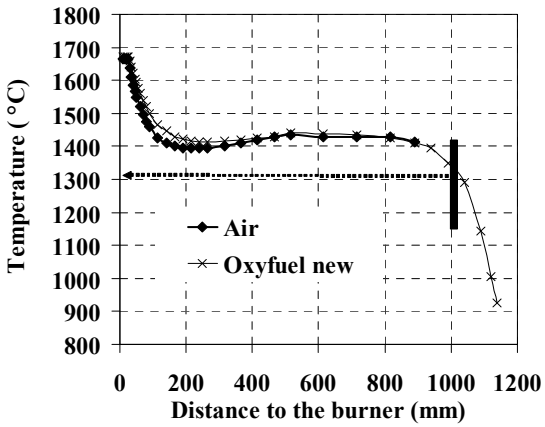

(b)

Figure 3.2 *(a) & (b) LCS temperature profiles*

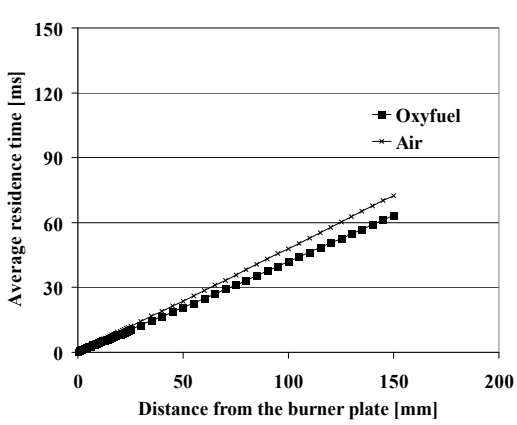

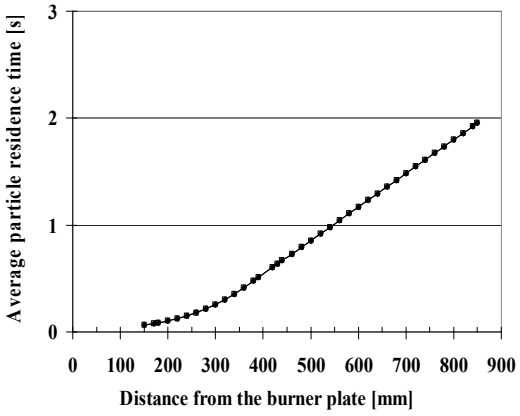

Figure 3.3 *LCS temperature profiles and b) residence times under air varying combustion conditions*

The residence times are also shown in Figure 3.3, both in the flame area close to the burner plate as well as along the reactor. Residence time calculations are based on the volume flows, the gas velocity, assuming laminar flow and taking into account the reactor geometry, axial gas temperature profile and the particle terminal velocity. We matched the volume flow rates in all cases, in both the inner and the outer burner, in order to have the same or very close volume flows. The selection of flows was such as to allow for the same residence times in all experiments for the given temperature profiles. A suction pump asisting constant volume flow rate also assures for homogeneous velocities and therefore isokinetic conditions in the reactor. The small difference in residence times in the burner area is due to the fact that flows were slightly adjusted in order to match the temperature profiles between air and oxyfuel combustion. Boiler tube fouling studies can be carried out using a horizontal probe placed at ~850 mm from the burner, simulating the gas/particles flow around a single boiler tube in the convective section of a boiler. It is provided with a ring shaped heat-flux sensor installed on the horizontal tube as well as with a detachable tubular deposition substrate. The surface temperature of the probe is controlled by the air cooling system and maintained at 660°C. It is supported that boiler retrofit to oxyfuel operation should be applied to modern and high efficient power plants, rather than to older and less efficient power plant units, in order to better amortize the large efficiency penalty after applying CCS measures. The surface temperature of the probe was chosen in order to include supercritical steam conditions, which is an option for oxyfuel applications. The effect of the surface temperature of the probe was not further studied in this paper and should be taken into consideration in future works.
Deposition samples can be collected in either the sensor area (sample No 1) or the detachable substrate (sample No 2). When the sensor is used, on-line data on the influence of the deposit on the effective heat flux trough the tube wall are collected allowing calculating the fouling factor, which is defined as the inverse of the overall heat transfer coefficient. The ash collected on the sensor is taken for ICP/AES analysis. It is also possible to collect ash on a detachable substrate and then fix the sample with epoxy for further SEM/EDS or other analysis. The remaining particles not deposited on the horizontal probe are collected through a vertically adjustable cooled probe at the end of the drop tube reactor on a porous filter (sample No 3), which is further submitted to ICP/AES analysis, together with sample No 1 from the horizontal ash deposition probe. The carbon in ash was also determined for all ash samples. The particle size distribution and the density of the ash samples collected in the horizontal probe and the filter were also determined. As it is a dilute system in terms of solids/gas ratio, compared with an autothermal full-scale PF furnace, the large volume of the surrounding flue gas kept at a constant temperature helps to maintain a relevant temperature on the surface of the char/ash particles, until the moment these reach a cooled surface of the deposition probe, avoiding inhomogeneous or too high peak temperatures in the char particles.
Deposition tests were carried out with the coals and their blends with biomass: Russian and African coal with cocoa residues at 20 % wt. and olive residue at 25% with lignite, combusted in O_2/CO_2, with a 30% vol. of oxygen in order to achieve the same adiabatic flame temperature and similar heat transfer characteristics than in air combustion. Proximate (ash, VM and moisture % (w/w) – oven / gravimetry) and ultimate analyses (C, H, N, O, S – Carlo-Erba analyser), as well as inorganic elemental composition using ICP/AES (29 elements in total) were performed on the fuels, the results shown in Table 3.1. The fuels were all ground to less than 500 μm: 250 μm < dp < 500 μm in order to be fed in the brush feeder. A series of combustion tests with Russian and South African coals and blends in air (79 % vol. N_2 and 21 % vol. O_2) were carried out as reference as well. In all oxyfuel condition test runs, in order to simulate flue gas recycling that will possibly contain, at least in traces, sulphur in the form of SO_x, a small volume flow of H_2S was added together with the fuel, which is oxidised immediately to SO_2/SO_3. It is still argued on the level of gas cleaning that has to be applied in the oxy-

fuel combustion; therefore defining the effect of a sulphur surplus on the deposition behaviour was considered important at this stage. Water vapour was not included in our tests, as part of the simulated recycled gas input, simulating dry recycling. Moisture in the recycled flue gas would increase the heat transfer coefficient of the flue gases even further, and this would possibly lead to a slightly lower recycling ratio in comparison with a dry recycling system, and a lower CO_2 concentration on the recycled flue gas. In the other referenced works there was no indication that steam vapour was added to the O_2/CO_2 stream either. In any case, gas cleaning prior to recycling implies that the gas is cooling down considerably in order to pass through the various gas cleaning devices. Finally, two tests (Russian coal in O_2/N_2 and in O_2/CO_2) were run using a cascade impactor (Pilat Mark V) in order to obtain size distributed ash samples and obtain insight into fine ash formation and composition under varying combustion environments (air and oxyfuel). Seven fractions in the size range >50 μm down to ~0.3 μm were obtained. Nuclepore polycarbonate filters were placed in the stage plates to allow subsequent microscopic analysis.
In order to provide specific data for the ADP model (Ash Deposition Predictor) some more tests were carried out in the LCS, Lignite and Russian coal combustion under air and oxyfuel conditions, in order to collect the whole ash produced in the filter at the reactor exit, avoiding splitting it into sensor and filter ash. The expected benefit will be the production of more accurate data for the simulations that are expected to give insight into the background that causes the observed variations in the test cases.

Table 3.1 *Chemical analysis of the used fuels*

Fuel	**Russian coal**	**Cocoa**	**South African**	**Lignite**	**Olive residue**
Moisture / Std Dev	3.4 / 0.5	11.1 / 1.4	3.9/ 0.3	35.8	5.78
Proximate analysis (% mass, dry fuel basis)					
ash @ 815°C / Std Dev	14.9 / 0.5	5.4 / 0.2	12.8 / 0.2	42.6	6.29
Volatile matter / Std Dev	29.0 / 1.1	61.9 / 1.3	25.3 / 0.3	38.1	72
HHV (KJ/kg) / Std Dev	27800 / 200	19410 / 80	28225 / 60	13700	20000
Initial Deformation (°C)	1250	1140	1350		
Hemisph. Temperature (°C)	1360	1310	1375		
Flow Temperature (°C)	1410	1330	1400		
Ultimate analysis (% mass, dry fuel basis)					
C / Std Dev	68 / 2	49.4 / 0.8	70 / 3	33	48
H / Std Dev	4.0 / 0.3	5.35 / 0.05	3.8 / 0.3	2.7	5.75
N / Std Dev	0.87 / 0.12	2.61 / 0.04	1.34 / 0.07	0.605	1.1
S / Std Dev	0.35 / 0.02	0.27 / 0.01	0.53 / 0.02	0.79	0.086
O by diff.	11.6	40.1	9.2	18.8	38
Ash composition (mg/kg fuel, dry basis)					
Na (± 7)*	405	179	269	1600	1300
Mg (± 1)	1277	1937	1665	5500	1800
Al (± 4)	16583	772	19794	34000	1200
Si (± 90)	34841	1861	21931	64000	6200
P (± 15)	386	1684	750	110	620
K (± 20)	2390	20790	790	6600	8900
Ca (± 20)	2750	2140	7500	7100	13000
Ti (± 8)	622	47	843	1400	76
Mn (± 6)	89	24	52	200	35
Fe (± 4)	6077	1095	2907	15000	1800
Zn (± 1)	21	4	10	50	12
Pb (± 20)	10	0	0	25	25
Sr (± 5)	183	18	454	59	15
Ba (± 5)	260	22	349	150	11
Cl (± 20)	100	800	50	47	2000

4. Results and discussion

4.1 Visual inspection data

In general, the ash deposited on the sensor and on the deposit substrate was loose and powdery and with the slightest movement the ash sample would fall off or diffuse in the air. In terms of colour and appearance the deposits did not vary between the various combustion conditions (oxyfuel vs air combustion). The deposit thickness difference however was profound amongst air and oxyfuel trials, the oxyfuel deposits being in general thicker. A thin white layer could be seen on the sides and bottom of some of the probes, possibly alkali chloride salts condensed onto the cool probe surface during the initial stages of deposit formation.

4.2 Ash deposition rates and deposition propensity

All ash samples collected in the horizontal probe during the deposition experiments as well as the filter ash samples were weighed. Several parameters have been introduced in order to assess the deposition tendency. First, the ash deposition ratio *DR* is calculated, which is defined as the ratio of the ash collected on the probe, $m_{dep,}$ to the fuel fed , m_{fuel}, both quantities measured directly.

$$DR = \frac{m_{dep}}{m_{fuel}} \tag{1}$$

Second, in order to normalise the ash deposition in relation with the fuel ash content, the deposition propensity *DP* is introduced, defined as the percentage of the ash collected on the deposit probe m_{dep} to the ash content in the fuel fed, m_{ash}. This ash content in the fuel is given by the proximate analysis of the fuel. The deposition propensity, here expressed in %, provides more insight into the inherent deposition characteristics of the different fuels, as it accounts for variations in fuel ash content.

$$DP = \frac{m_{dep}}{m_{ash}}(\%) \tag{2}$$

Figure 4.1 shows the deposition ratio and the deposition propensity as defined for the various test runs. This graph includes results from all 3 mentioned testing periods.

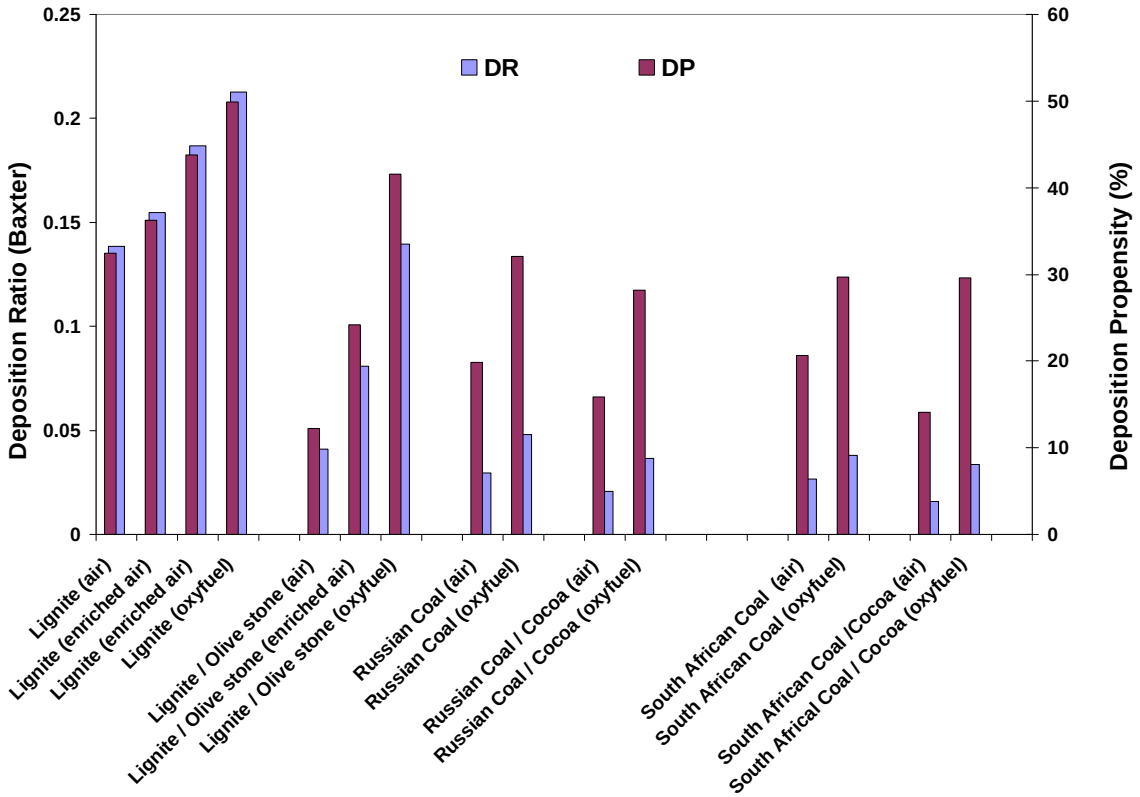

Figure 4.1 *Deposition Ratio and Deposition Propensity for the fuels and blends combusted in air and O_2/CO_2*

As mentioned, the system is dilute in terms of solids/gas ratio. The flame temperature is controlled by the flat flame gas burner, and the temperature profile in the reactor is controlled by external heaters. The main flue gas flow and composition are formed and controlled by the methane and oxidant streams introduced by the staged burner. The low particle feed rates are used in order to control the gaseous environment of each particle by means of the imposed gas burner conditions. Therefore the influence of a 20% replacement of the solid fuel (coal) by biomass, on the total heat release and oxygen demand is insignificant.

It can be seen that the deposition ratio (Fig. 4.1) is, as expected, increasing with the ash content of the fuels as shown in Table 3.1, and it can be observed that the deposition ratios are lower under air combustion. The coals studied present in general lower deposition propensities (Fig. 4.1) when they are blended with biomass, probably due to ash elements interactions e.g. Cl present in the biomass forming compounds that enter the gas phase. The deposition propensity is a direct indication of the ash stickiness, lower propensity means lower stickiness.

The ash collected in the deposition probes for the different experiments were always easy to detach from the probe being a loose powder. The carbon in ash in the samples was measured, confirming that the higher deposition of the oxy-fuel samples was not due to unburnt fuel particles that might be present in the deposits. Carbon - In -Ash values are shown in Table 4.1, where it can be seen that there a fluctuating carbon percentage in some of the tests. If the C% in the ash is high, it could affect the deposition ratio which seems then higher, but not due to ash deposited but due to carbon deposited. This of course would be misleading and needs to be considered carefully.

However this tendency was not systematic in our tests, and at some cases higher carbon in ash was observed in the air cases and some in the oxyfuel cases, not affecting though the systematic deposition behaviour. Furthermore, during the tests we also monitored the CO_2 and O_2 levels in the exit together with the flue gas composition at the exit. The CO levels were always low, slightly higher than the levels of CO emissions when the reactor operated on the methane (pilot) flame without fuel, indicating satisfactory combustion, not loading the deposited ash with high loads of carbon particles.

A final issue possibly affecting ash deposition behavior is the flame temperature profiles in the two combustion conditions; it can be the case that although the tip flame temperature is approximately the same under oxyfuel and air conditions, the flame length is somewhat larger in the oxyfuel case, as implied by a higher temperature profile, and therefore the particles are exposed to higher temperatures during a longer time (Figure 4.2). Variations in exposition times or peak flame temperatures might indeed lead to variations in 'sticky' mineral matter amounts which are likely to agglomerate, producing ash particles that are coarser and more prone to deposition. In our tests indeed, some of the particles' rounded shape observed in the microscope for both the oxy-fuel and air samples, indicates that the ash was exposed to temperatures reaching the theoretical melting temperature of some of the ash compounds. However we did not observe slag in the sensor and deposit samples when extracting the probe from the reactor, which would imply fluxing ash melt, as the material was powdery and easy to blow off.

Table 4.1 *Carbon in ash and flue gas composition for the test cases*

Fuel blend	**C in ash (w/w %, dry) Deposited / filter**	**Flue gas at the exit (CO_2 %, O_2 %, CO ppm)**
Russian Coal (air)	1.75 / 1.07	10% / 3.0% / 14 ppm
Russian Coal (oxyfuel)	2.57 / 0.8	87% / 2.5% / 22 ppm
Russian Coal / Cocoa (air)	7.6 / 0.2	9.5% / 2.5 % / 16 ppm
Russian Coal / Cocoa (oxyfuel)	2.17 / 0.76	86% / 3.0% / 25 ppm
South African Coal (air)	6.7 / 0.98	9.5% / 2.8 % / 20 ppm
South African Coal (oxyfuel)	10.1 / 1.02	83% / 2.8% / 30 ppm
South African Coal /Cocoa (air)	6.8 / 1.22	9.5% / 3.0 % / 15 ppm
South African Coal / Cocoa (oxyfuel)	2.73 / 0.87	85% / 2.8% / 21 ppm
Russian Coal (air) *Cascade Impactor*	Not detected	10% / 3.3% / 4 ppm
Russian Coal (oxyfuel) *Cascade Impactor*	Not detected	83% / 3.6% / 0 ppm
Lignite (air)	0.26 / 0.12	10% / 3.4% / - ppm
Lignite (enriched air)	0.12 / 0.10	45% / 3.0% / - ppm
Lignite (oxyfuel)	0.12 / <0.10	86% / 3.9 % / - ppm
Lignite/olive (air)	0.18 / 0.13	9.9% / 3.5% / - ppm
Lignite/olive (enriched air)	0.12 / 0.10	46% / 2.8 % / - ppm
Lignite/olive (oxyfuel)	0.15 / <0.10	87% / 3.7% / - ppm
Lignite (air) duplicate	0.26 / 0.10	9.5% / 3.7% / - ppm
Lignite (oxyfuel) dupl.	0.1 / 0.1	86% / 4.2% / - ppm
Russian Coal (air) dupl.	1.67 / 5.64	9.8% / 3.7% / 5 ppm
Russian Coal (oxyfuel) dupl.	0.9 / 5.79	85% / 4.5% / - ppm

An explanation of the observed differences in the ash deposition propensities is attempted considering the deposition mechanisms: inertial impaction including impaction and sticking, thermophoresis, condensation and chemical reaction [63]. Inertial impaction is prevailing in reactors as the present one, dependent on the variations in the physical gas properties, as e.g. the gas density of CO_2/O_2 mixture, which is higher than under N_2/O_2 conditions. Therefore, we identify two possible reasons for the higher deposition behaviour under oxyfuel combustion.

1. Larger ash particles may be formed, leading to increased inertial impaction onto the deposition probe. The reason for the larger particles may well be a local high tem-

perature (peak) due to higher oxygen concentrations that increase the char combustion temperatures locally without affecting the overall temperature profile.
2. Gaseous properties are different, as the CO_2 is denser and has different viscoelastic behaviour. This leads probably to changes in the flow field (velocities, particle trajectory) that leads to the observed effects.

Another remark concerning inertial impaction in our reactor is that the deposits were found predominantly on the front side of the tube, as the deposition probe is placed in cross flow, promoting the collision of the particles in the front area. In addition, there was no deposition built up on the sides of the probe or even less on the down stream side of the probe, except of a thin layer of fine ash at the sides. This verifies the absence of ash slag and the presence of possibly other ash deposition mechanisms on our sampling rig, less dominant than inertial impaction, e.g. thermophoresis. A thin film formed by the alkalis condensing on the surface might have aided the formation of a first ash particle layer upon which the deposit started growing due to inertial impaction.

At this point though it must be mentioned that the effect of increased CO_2 partial pressure on carbonates formation ($CaCO_3$, $FeCO_3$) was not studied, which might give a hint on the deposition behavior observed. This issue was studied with X-Ray diffraction XRD (metallographic analyses and the results are presented and commented upon at a later paragraph.

Therefore, we concluded that the systematic differences in the deposition behavior of the same blends under the two combustion conditions is due to the differences in the flow fields and in the physical properties (density, viscosity) of the gaseous mixtures. However we suspect that the ash particle size plays an important role in the deposition behaviour, as the particle size affects the inertial impaction behaviour of the ash on the sensor.

The filter (fly) ash, collected at the reactor exit, preventing the analytical instruments, is the residual ash not captured in the deposition probe surface. After performing an ash mass balance, Figure 4.2a shows the filter ash percentage compared to the total ash fed:

$$ash(\%)w/w = \frac{m_{filter.ash}}{m_{total.ash}} \quad (3)$$

which is the ratio of the ash collected in the filter $m_{filter.ash}$, to the fuel ash fed $m_{total.ash}$. In order to directly compare the distribution between the deposited ash and the ash collected in the filter for the two combustion environments, these two quantities are expressed as percentages of the total ash fed, shown in Figure 4.2b which shows the ash distribution percentages under air and oxyfuel conditions, between the deposited and filter ash in relation to the total fuel ash. The ash balance did not add up to 100%, but it was in all cases somewhat lower, around 90%.

Given the fact that the fuel mass flow rate, the quantities fed and the fuel particle size distribution is the same under air and oxyfuel conditions, together with the information on deposition ratio and propensity shown in Figure 4.1, we can conclude that the ash deposition behaves differently between air and oxyfuel combustion. Less amount of ash deposited for the air case is observed together with a higher amount of fly ash found back in the filter, in comparison with the oxy-fuel conditions.

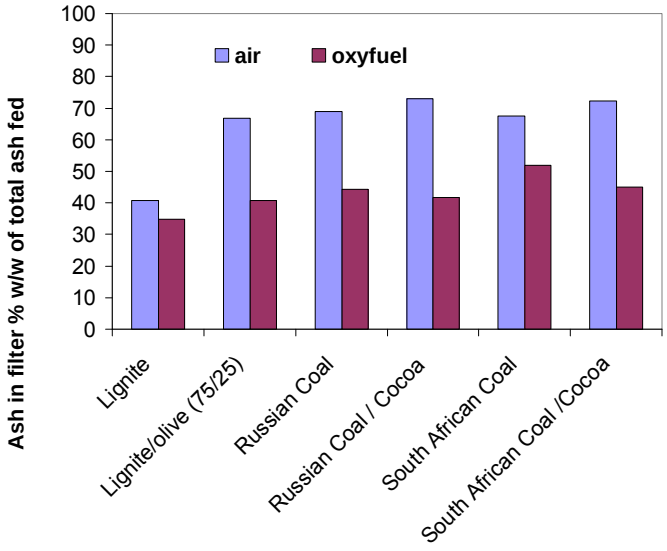

(a)

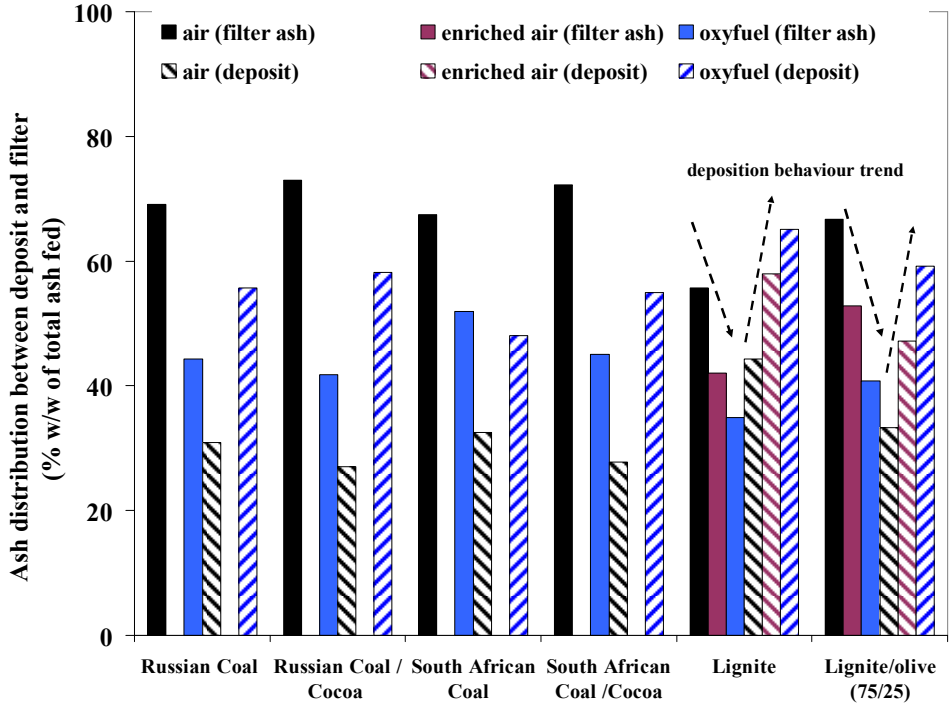

(b)

Figure 4.2 *(a) Filter ash deposition ratio and (b) Ash distribution between deposit and filter ash for the fuels and blends combusted in air, enriched air and O_2/CO_2*

Transferring the deposition behaviour observations into the full-scale is not straightforward, however. The LCS is a down-fired entrained-flow drop-tube-like test rig, in which all the particles, independent of the size and composition will end up at the bottom, where the sampling train is located, and in the filter ash. In a full-scale power plant, opposed-, tangentially or down-fired, the prevailing deposition mechanisms are more complicated, affecting the ash distribution. However, the conclusion that under oxyfuel conditions systematically less fine ash was found back in the filter (fly ash) and more coarse ash was deposited, as opposed to the air case, can prove useful in the design

of the heat exchanger tubes and surfaces generally, preventing excessive fouling in points that were not considered under conventional air operation. More information is necessary in order to make clear practical conclusions, gained from testing different fuels that will produce various particle size distributions of ash and simulations of ash deposition using computational fluid dynamics (CFD) in order to evaluate the observed results.

4.3 Fouling factor calculation

Based on the heat flux data measured on-line by the sensor probes the so called fouling factor R_f of the obtained deposits can be estimated, which corresponds to the ash deposits heat transfer resistance:

$$R_f = (\frac{1}{U_1} - \frac{1}{U_0}) = \frac{T_g - T_c^1}{HF_1} - \frac{T_g - T_c^0}{HF_0} \quad (4)$$

where:
R_f – fouling factor, (K·m^2)/W (heat transfer resistance)
U_1 – ash deposits heat transfer coefficient after time $t=t_1$, W/(K·m^2)
U_0 – initial heat transfer coefficient after $t=t_0=0$, W/(K·m^2)
T_g – flue gas temperature, K,
T_c – coolant medium temperature inside the deposition probe, K,
HF_1 – heat flux to the sensor after time $t=t_1$, W/m^2,
HF_0 – initial heat flux to the sensor $t=t_0=0$, W/m^2.

The fouling factors of the Russian & South African coals with cocoa and the Lignite with olive residues are depicted in Figures 4.3 a & b as an almost linear function of the cumulative ash feed rate. The slopes of the curves plotted become independent of the fuels' various ash contents. The point at which fuel feeding started was taken as the beginning of the heat flux measurement. In all cases the heat flux, surface temperatures, cooling air flow rate and furnace temperatures reached steady state by the start of the deposition measurement.

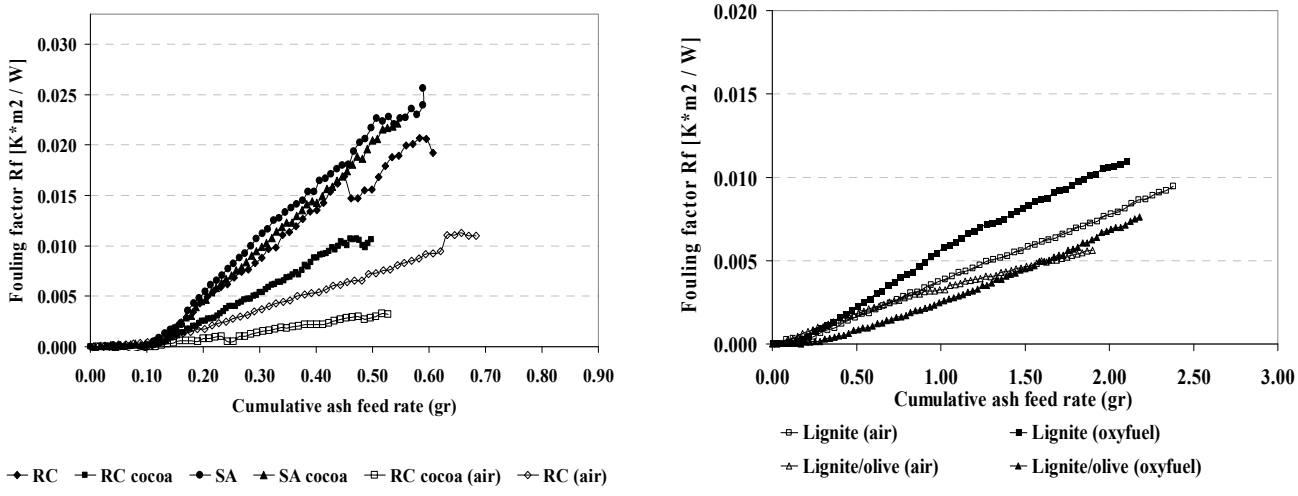

Figure 4.3 *Calculated Fouling factors versus accumulated feed rate for the tested blends under air and oxyfuel conditions. RC = Russian coal, SA = South African coal*

The coal/cocoa blends show lower fouling factors than the coals, in accordance with the deposition propensity results. However, it has to be noted that generally a higher deposition propensity does not always imply that the fuel has a higher fouling propensity; other factors like the thermal conductivity of the deposition layer or the scattering of the deposit on the probe, in other words the deposit density, might also play a role in the heat transfer properties of the deposition layer, affecting therefore the fouling factor value. Therefore, there is a difference in the scale between the two presented test runs, due to the variation on the physical properties of the formed ashes that care derived from different fuels.

4.4 Chemical composition analysis: Element enrichment - ICP analyses of deposited and fly ash

The behaviour and distribution of the ash elements was defined and quantified by performing a mass balance including the weights and inorganic compositions of the fuels and ash samples obtained from (1) the deposited ash, which resembles the bulk ash and (2) the fly ash, obtained from the filter, which contains the ash that was not deposited on the probe.

The results of the elemental composition of the deposited and filter ash are presented using the enrichment factor *EF* which describes the relative enrichment of an element in the sampled ash relative to its concentration in the fuel ash. The enrichment factor *EF* is defined for either the deposited ash or the filter ash as

$$EF_i = \frac{X_{dep,i}}{X_{ash,i}} \tag{5}$$

where $X_{dep,i}$ is the mass fraction of the element *i* (expressed as oxide) in either the deposit or the filter ash and $X_{ash,i}$ is the mass fraction of the element *i* (expressed as oxide) in the initial ash of the fuel prior to combustion. The results for the various test cases are given in Figure 4.4a – e, and will be commented upon in the following paragraphs.

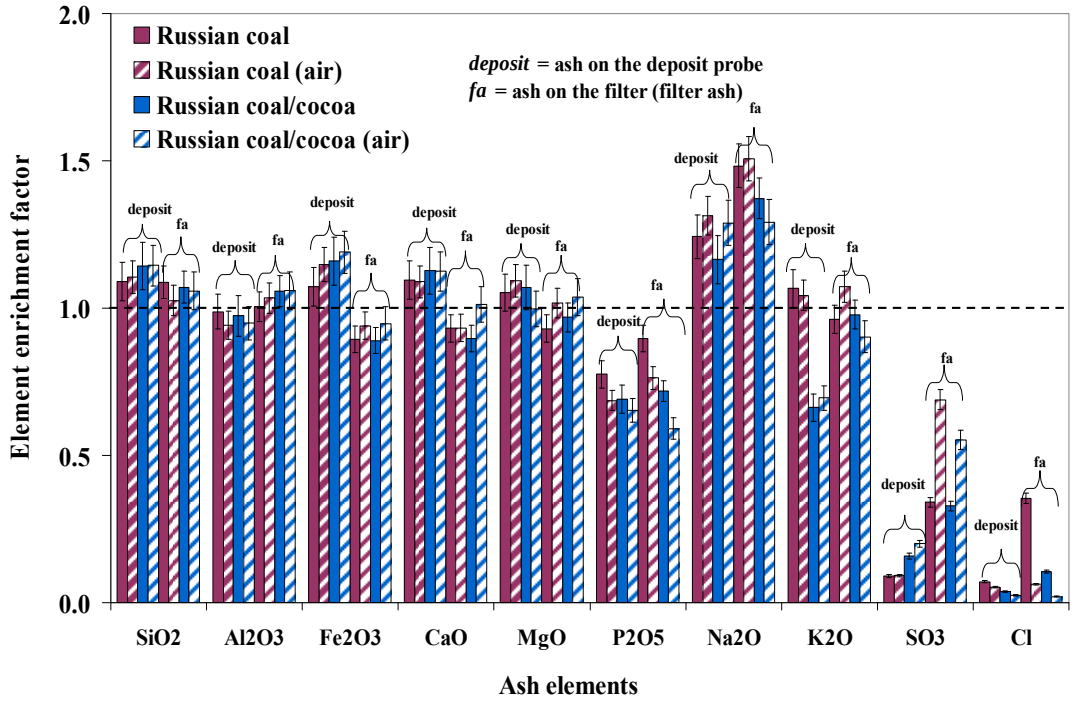
Russian coal
Russian coal (air)
Russian coal/cocoa
Russian coal/cocoa (air)
deposit = ash on the deposit probe
fa = ash on the filter (filter ash)
Element enrichment factor
2.0
1.5
1.0
0.5
0.0
deposit
fa
SiO2
Al2O3
Fe2O3
CaO
MgO
P2O5
Na2O
K2O
SO3
Cl
Ash elements

(a)

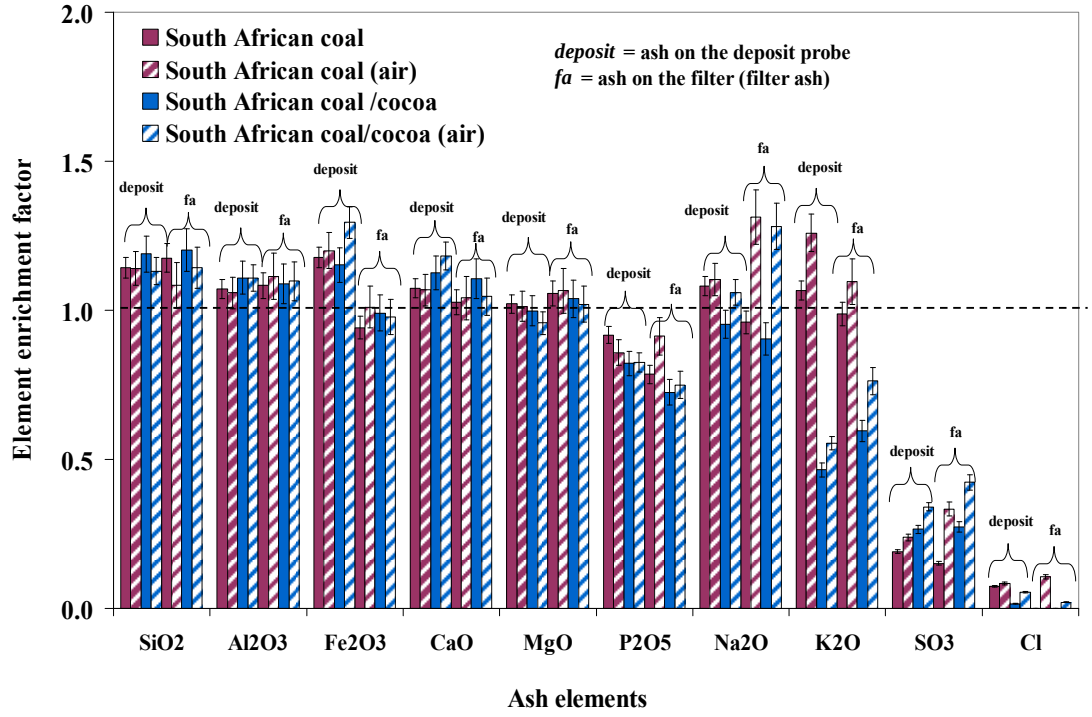
South African coal
South African coal (air)
South African coal /cocoa
South African coal/cocoa (air)
deposit = ash on the deposit probe
fa = ash on the filter (filter ash)
Element enrichment factor
2.0
1.5
1.0
0.5
0.0
deposit
fa
SiO2
Al2O3
Fe2O3
CaO
MgO
P2O5
Na2O
K2O
SO3
Cl
Ash elements

(b)

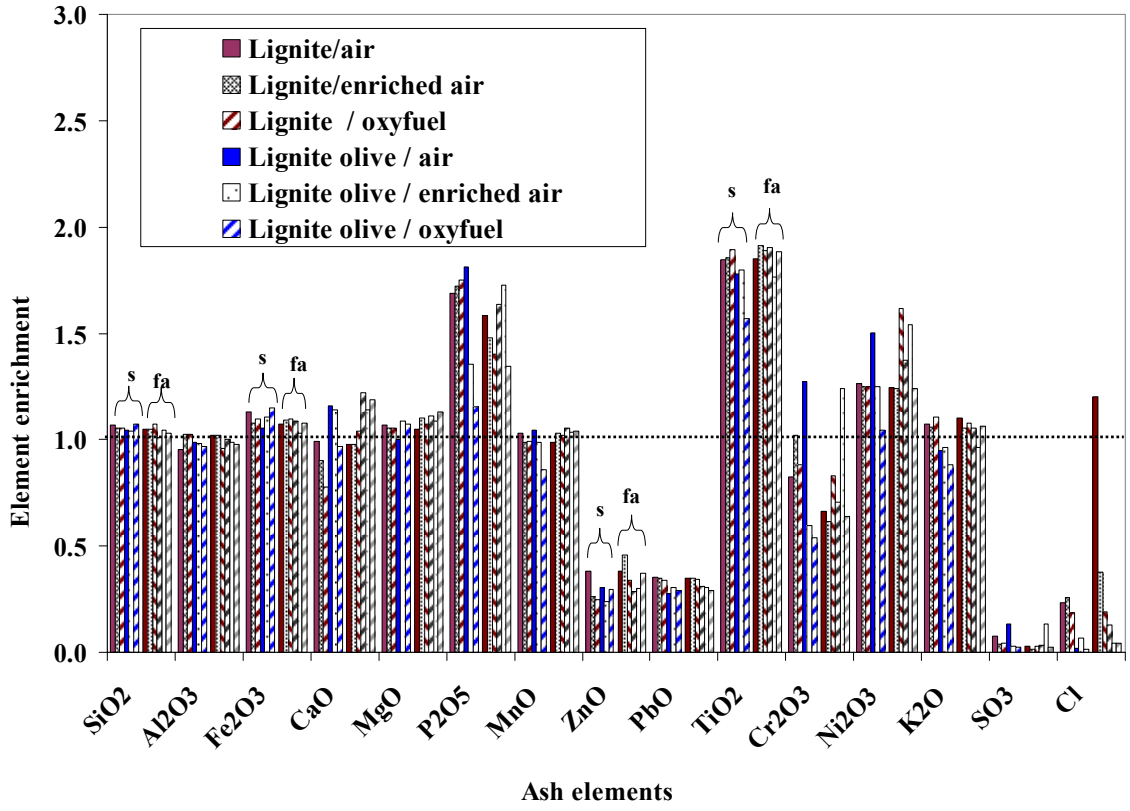
Lignite/air
Lignite/enriched air
Lignite / oxyfuel
Lignite olive / air
Lignite olive / enriched air
Lignite olive / oxyfuel
Element enrichment
3.0
2.5
2.0
1.5
1.0
0.5
0.0
s
fa
SiO2
Al2O3
Fe2O3
CaO
MgO
P2O5
MnO
ZnO
PbO
TiO2
Cr2O3
Ni2O3
K2O
SO3
Cl
Ash elements

(c)

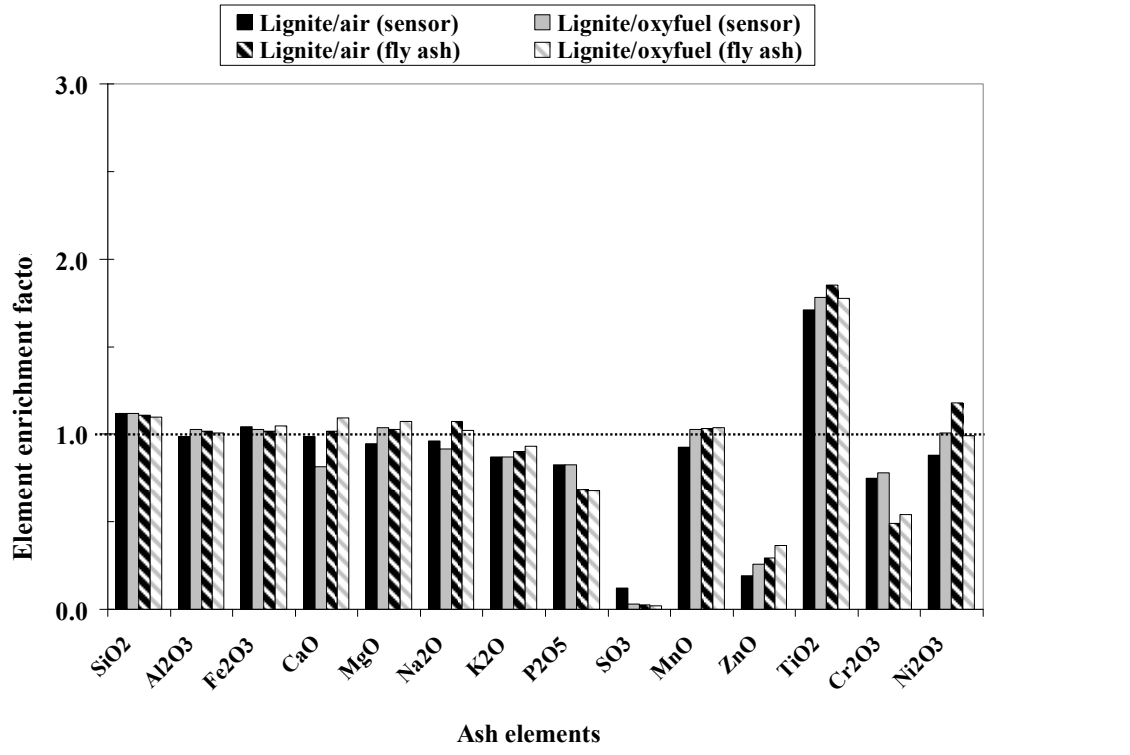
Lignite/air (sensor)
Lignite/oxyfuel (sensor)
Lignite/air (fly ash)
Lignite/oxyfuel (fly ash)
Element enrichment facto
3.0
2.0
1.0
0.0
SiO2
Al2O3
Fe2O3
CaO
MgO
Na2O
K2O
P2O5
SO3
MnO
ZnO
TiO2
Cr2O3
Ni2O3
Ash elements

(d)

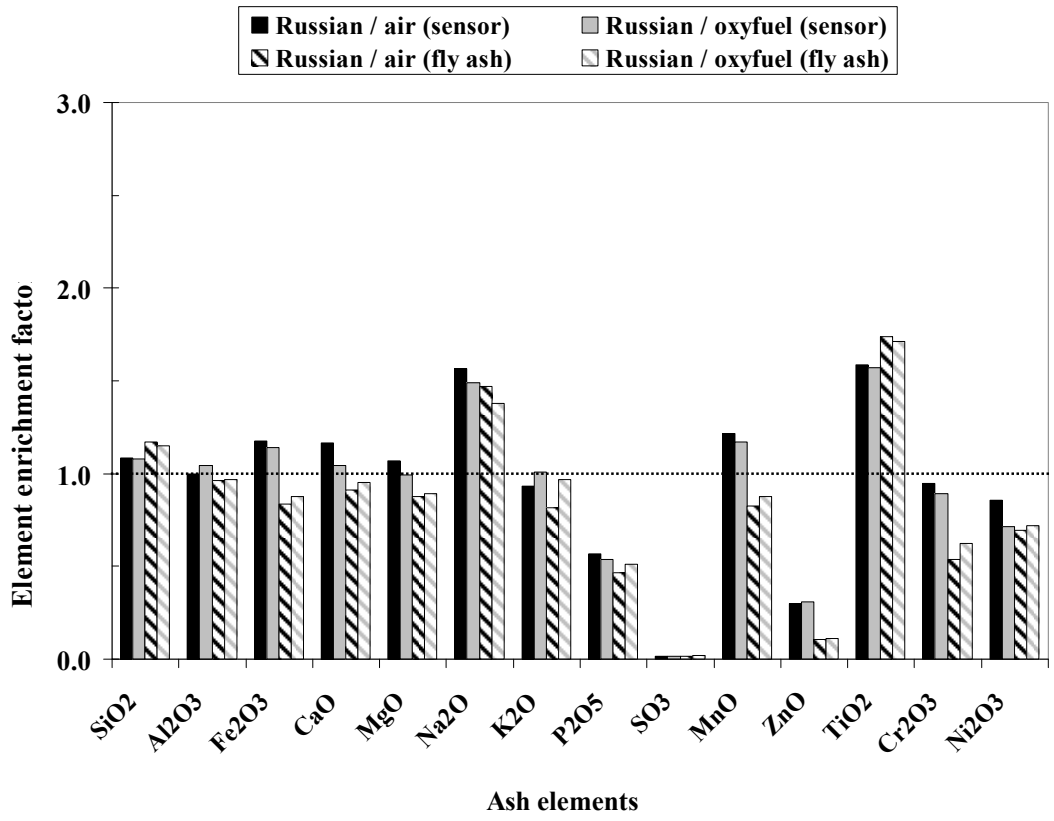

(e)

Figure 4.4 *a - e: (a) Element enrichment in the sensor (deposit) and filter ash for the Russian coal blends in air and oxyfuel (b) Element enrichment in the sensor (deposit) and filter for the South African coal blends in air and oxyfuel (c) Element enrichment in the sensor (deposit) and filter for the Lignite blends in air and oxyfuel (d) Element enrichment in the sensor (deposit) and filter for the Lignite and (e) Russian coal in air and oxyfuel (duplicate test)*

It can be observed that for the coal/biomass blends the ash collected from the deposit probe is slightly depleted in potassium, as observed by other investigators [64]. This indicates that potassium enters the gas phase either due to the chlorine (Cl) present which is increased in the case of the Cl-rich cocoa blends, facilitating the volatilization of elements that would otherwise deposit [65] or simply due to the fact that K in the biomass ash is more reactive, and therefore mobile, compared to coal ash K. In that case the slight decrease in *EF* is just due to the biomass addition, not implying biomass - coal ash interactions. This could in any case explain the relatively lower deposition propensity of the coal/cocoa blends. However, the filter ash does not seem generally depleted in K, as observed for the Russian coal/cocoa blends. In other published works, e.g. [66], the increased Cl input is observed to lead to an increased K concentration in the fly ash, because it mobilizes the K, forming KCl which ends up either in the fly ash or condenses on the cold surfaces. The released KCl can condense on cold surfaces after the filter, as for example in our facility, on the glass capillary part of the membrane pump used for the gas sample into the gas analysis device, where a white film was observed after the blends experiments. Due to the very small sodium concentration in the fuel ash it is not safe to draw conclusions on its behaviour.

All the deposit samples show almost complete chlorine depletion, as also reported in other works [67]. This indicates that Cl is released in the gas phase probably as HCl

(and to a smaller degree as KCl) which might be found back in the fine ash (filter ash sample) or just pass through the filter without condensing. An exception is observed though in the fly ash samples of the Russian coal but in general Cl was detected in very low concentrations implying its volatilization. Another published work [68] also reported that NaCl and KCl become unstable and are not found in deposits at temperatures higher than 650˚C.

Also S is depleted in both the deposit as well as the filter ash, as it is suggested to react with alkalis and therefore enters the gas phase [57]. Under high temperatures and oxidising conditions, essentially all of the sulfur-containing inorganic species in coal (primarily sulphates and pyrites) decompose to form SO_2 therefore none of the fuel sulphur passes unreacted through the combustor [65]. At the deposition probe temperature at 660^{o}C, some of the gaseous SO_2 reacts with alkaline earth and, to a lesser extent, alkali oxides and salts to form sulphates. Cocoa introduces some amount of Ca which could react with S into $CaSO_4$, which is a solid phase and also prone to deposit. This might explain the slightly higher S enrichment of the deposited ash of the coal/cocoa blends, but this is not observed for the filter ash of the Russian coal/cocoa blend, neither in the Lignite and Lignite / biomass cases. However, the relatively small sulphur concentration and the high Si/Al content of the fuels ash leads to the conclusion that most of the potassium and sodium in the deposit is expected to form alkali aluminum silicates rather than bind with S. Alkalis seem to remain in the ash instead of entering the gas phase (*EF* about 1). The increase of S enrichment and at some points of Cl in the fly ash, in comparison with the deposited ash, could be explained by considering condensation of gaseous phase elements on the finer fly ash which is caught by the filter. Such a conclusion however cannot be extracted for the alkalis, which show a relatively constant *EF* between deposited and filter (finer) ash.

Phosphorus *EF* values are similar for the various fuels' and blends' ashes and combustion conditions, with values slightly lower than 1. The other elements (Si, Al, Fe, Ca, Mg) show an *EF* ~1.

A major conclusion here is that a clear effect of the combustion environment, air vs. oxyfuel, on the *EF* results is not observed for the coals and their blends. Further work is needed in order to draw final conclusions.

As for the other elements (Si, Al, Fe, Ca, Mg), the *EF* is constant in all cases; therefore neither the combustion conditions nor the blends seem to affect the deposited or the filter ash enrichment.

4.5 Chemical composition analysis: Element enrichment - ICP analyses of size resolved ash samples

Size resolved ash samples using a cascade impactor (staged filter) were collected during the combustion of Russian coal and Lignite in air and O_2/CO_2. The ash samples collected at the different stages of the impactor were weighed, subjected to ash composition analysis and observed with scanning electron microscopy (SEM/EDS). An effort is made in this section to obtain further insight into the effect of the combustion conditions, air and oxyfuel, on the release of elements in the fine ash and a comparison and evaluation of the observed results with results reported in the literature is attempted.

The enrichment factors *EF* of the main volatile elements in each stage, expressed as oxides, is shown in Figures. 4.5 a - d. The advantage of the ICP ash analysis is the chlorine and carbon - in - ash detection, which is not possible to be detected in the

SEM/EDS, however for very small quantities of ash, as in the fine ash stages (bottom stage) the use of SEM/EDS is preferred as ICP cannot be applied. Therefore the results have been evaluated carefully taking into account all analyses.

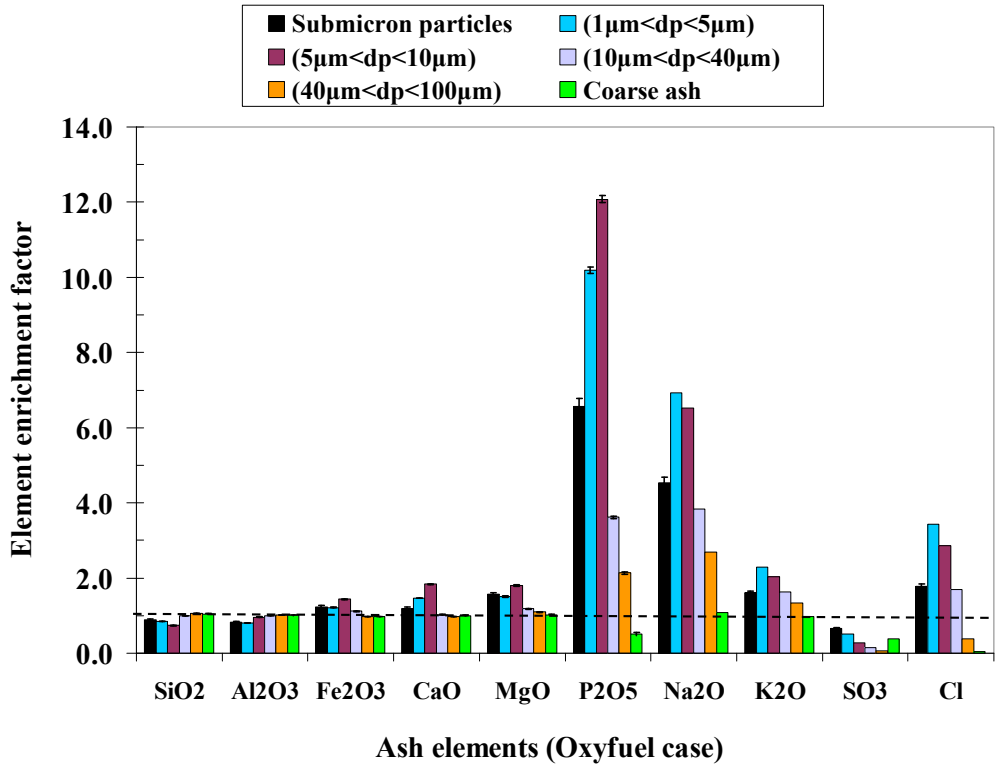

(a)

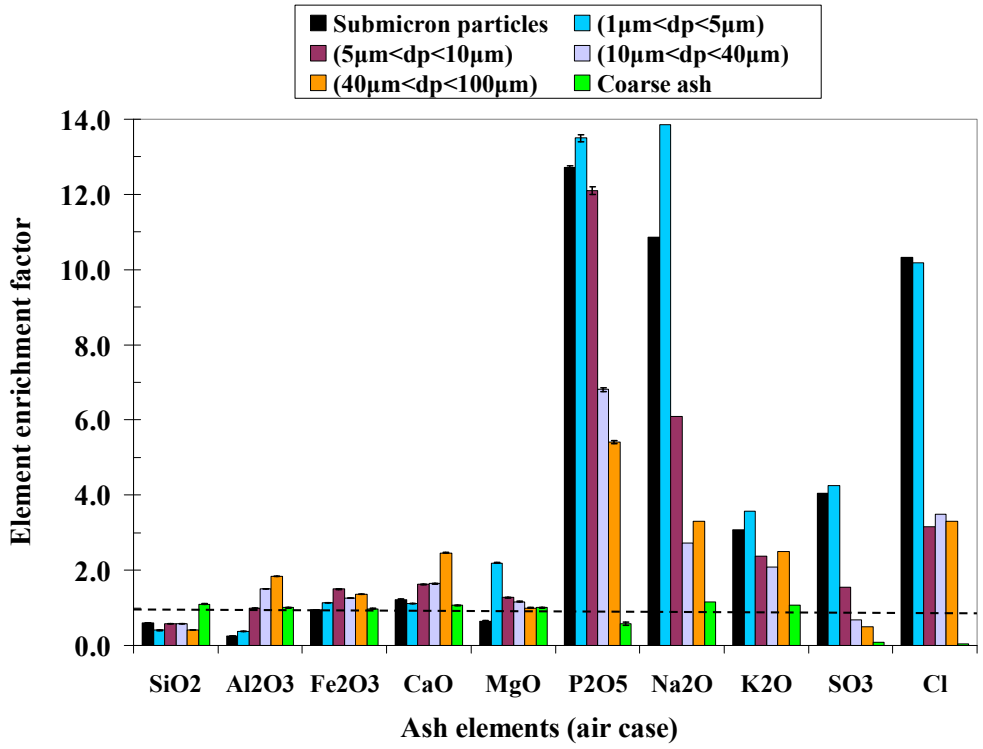

(b)

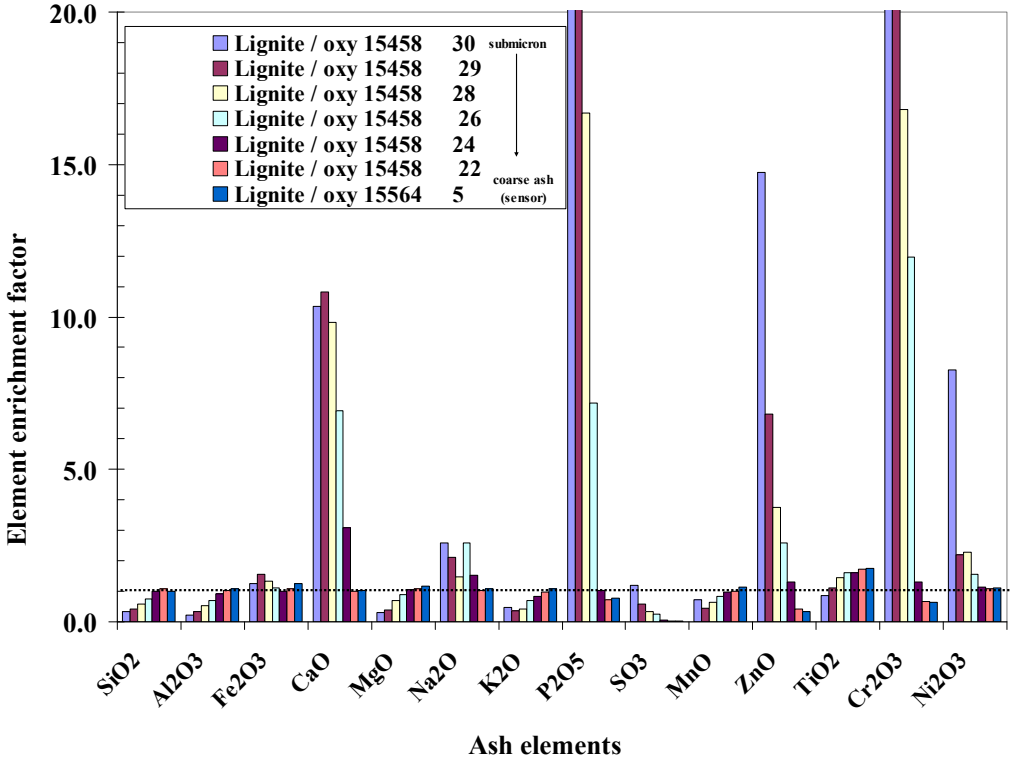

(c)

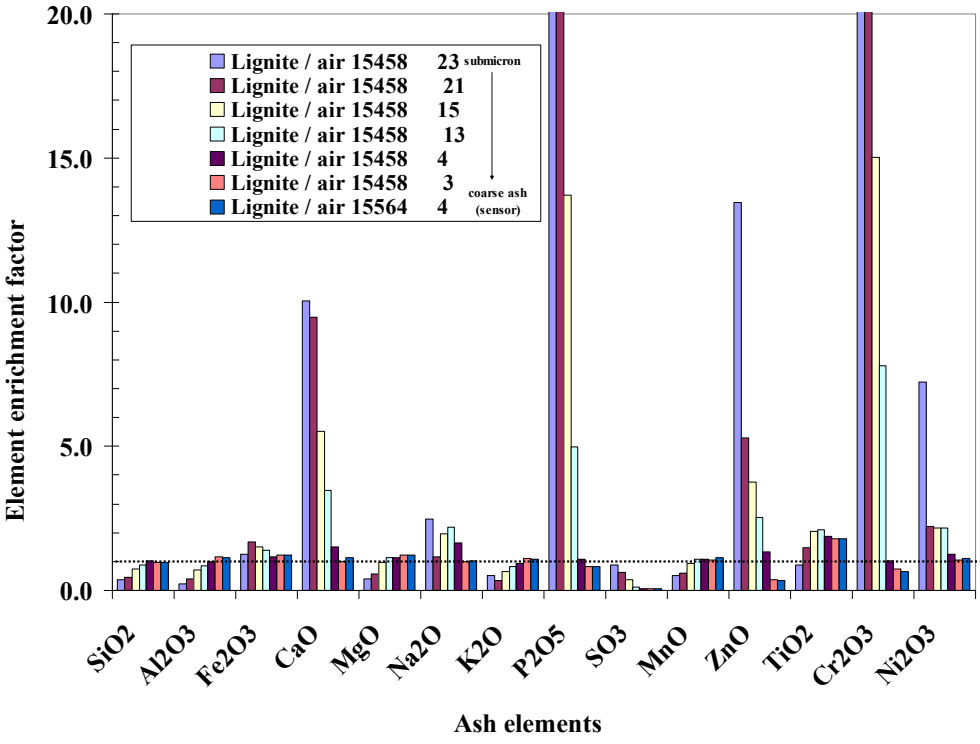

(d)

Figure 4.5 *(a) Element enrichment in the fine ash under oxyfuel conditions and (b) Element enrichment in the fine ash under air conditions.* ***Fuel:*** *Russian coal (c) Element enrichment in the fine ash under oxyfuel conditions and (d) Element enrichment in the fine ash under air conditions.* ***Fuel:*** *lignite*

It is observed that the concentration of certain elements (P, Na, K, S, Cl) in the finer ash stages is increased in relation to their percentage in the larger particle size area, in both air and oxyfuel conditions. This could be explained by vaporization and subsequent condensation of volatile elements on the fine ash particles, as also observed and reported in other publications [57], [69]. In [70] it is stated that the size dependent chemical composition of the submicron ash indicates that the condensation of evaporated species was responsible for the formation of ash particles smaller than 0.3 μm. The lower concentrations in refractory oxides are due to a limited vaporization rate of these elements (including SiO_2, Fe_2O_3). In the case of Lignite however, the concentration of CaO in the submicron scale were unusually high. This is maybe due to the high Ca content of Lignite, which forms very fine ash as it fragments.

Even if only a small fraction of alkalis, Cl and S of the initial fuel ash is found in the gaseous phase, it is sufficient to produce a certain amount of submicron particles of which the inorganic (elemental) composition is quite different from the bulk fuel ash composition. This is due to the different ash formation mechanisms that determine the submicron ash formation, which is mainly condensation and nucleation of volatilised ash elements, as opposed to fragmentation of original mineral inclusions that define the formation of larger ash particles. Therefore the enrichment in S and K in the submicron ash does not seem in accordance with the tendency shown in Figure 4.4, showing *EF* values around 1 or less (depletion), however the submicron ash particles constitute a small fraction of the total ash produced and therefore do not change considerably the bulk ash composition.

Considering Figure 4.5, the *EF* values for the coarse particles converge to the values shown in Figures 4.4. The differences in the *EF* values are diminished above a certain particle size for both combustion conditions, as the mechanism of ash formation for larger ash particles is not due to nucleation and condensation anymore, but as mentioned before, mainly to fragmentation. A change in the fine ash chemical composition between air and oxyfuel combustion can be observed, despite the fact that the bulk ash compositions do not show significant differences in the two cases.

In conclusion, it is not clear whether the oxyfuel ashes are more enriched in refractory elements (higher *EF* values for Ca, Si, Fe, Al, Mg, P). Therefore it cannot be concluded that the variation in the combustion conditions affect the release and initial vaporization of volatiles and refractory species in the initial stages of combustion, due to the changing ratios of O_2, CO_2 and CO within the burning char particles. This has been supported by others [54, 49, 56], where it is concluded that the gas environment, namely the relative O_2/CO_2 ratio in the oxidant mixture or the CO/CO_2 ratio in the char, affects the local char combustion temperature, the local heat transfer conditions and therefore the vaporization of elements, volatile or refractory. As indicated in [56], the increasing CO_2 in the bulk gas changes the CO/CO_2 ratio in the char particle, which could affect the vaporization of refractory oxides from the fuel char, and consequently impacts the formation of fine ash particles. This could however explain the higher concentration of SiO_2 or Al_2O_3 in the finer oxyfuel ash in the test runs including Russian and South African coals. From our experiments we conclude that oxyfuel combustion, as compared to air combustion, does not seem to affect the ash chemistry or the general mechanisms of ash formation (degree of condensation or fragmentation). Local temperature variations or the relative local $CO/CO_2/O_2$ ratios can affect the release of inorganic volatile or refractory elements, and affect therefore the composition of the fine ash material. The overall deposition behaviour is not affected by this different elements release between air and oxyfuel conditions, but by the different flow fields and flue gas composition in the furnace between air and oxyfuel combustion. This is studied in Part II.

4.6 Ash particle size distribution

Another observation concerns the particle size distribution of the produced ash between air and oxyfuel conditions. Some of the measured Particle Size Distribution (PSD) values are shown in Figure 4.6. At this point it must be stressed out that the PSD was determined for the sensor ash and separately for the fly ash. This introduces some uncertainty in the final conclusions, therefore dedicated tests were done in order to collect the ash from the combustion of the fuels under the investigated conditions, without the horizontal probe, in other words without dividing the ash into sensor (coarse) and fly ash (finer). This is called in the Figure below 'whole ash sample.

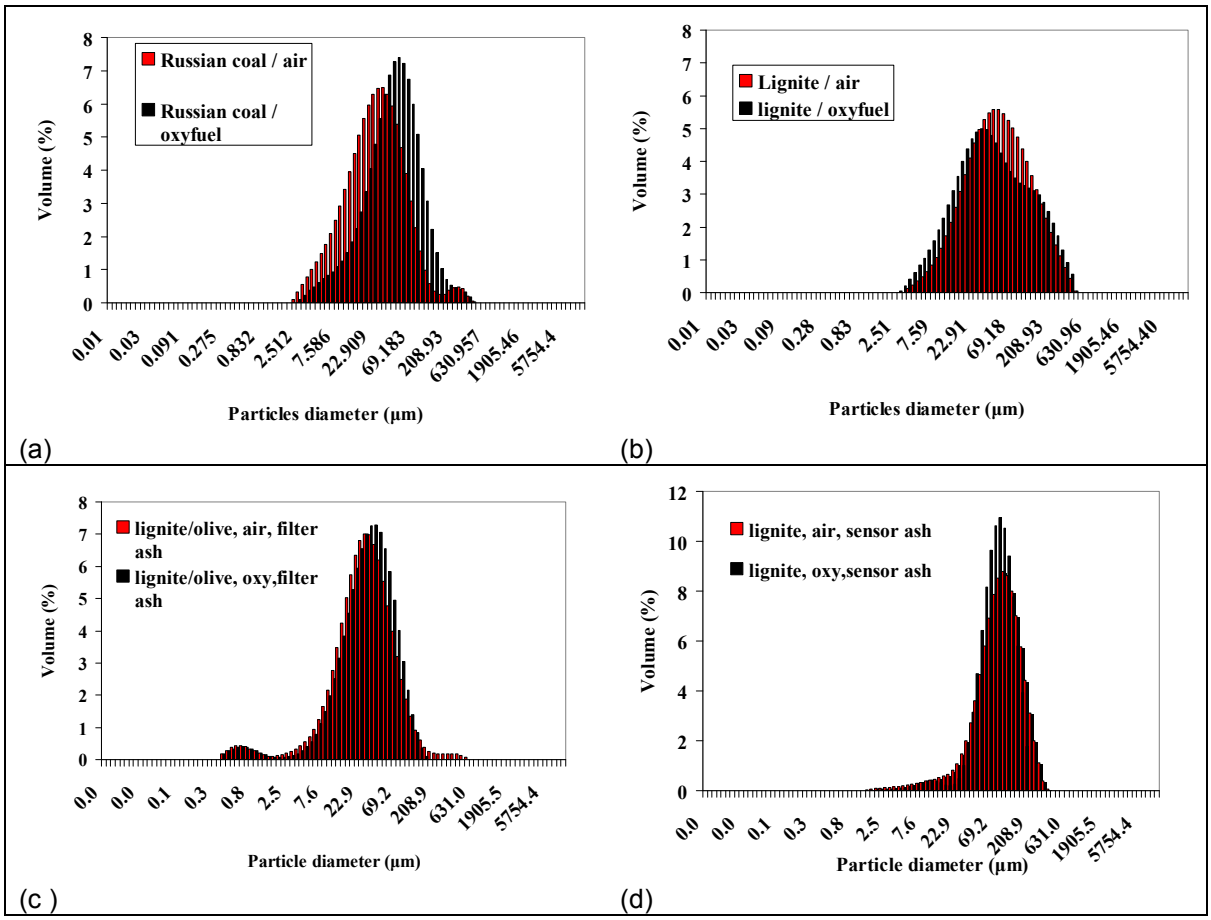

Figure 4.6 *Particle Size Distribution for selected test cases (a) Russian coal under air and oxyfuel (whole ash sample) (b) Lignite under air and oxyfuel (whole ash sample) (c) Lignite/olive under air and oxyfuel (only filter ash) (d) Lignite under air and oxyfuel (only sensor ash)*

In general, a larger average particle size was observed under oxyfuel conditions, which could be linked to the increased deposition rates under oxyfuel conditions, because it is expected that larger particles are more prone to directly impact on the deposit surface. However, there were several cases where the average particle size was not clearly larger in the oxyfuel case, but also in cases not shown here, and the deposition ratio and propensity under oxyfuel was still larger.

Therefore, the particle size is definitely a parameter to consider, but does not seem to be the only factor influencing the deposition behaviour. Also the viscous-elastic properties of the gaseous blend is suspected to affect the deposition behaviour, and finally, the flow fields itself (velocity vectors and particle trajectories).

Finally, the blends have shown a lower deposition tendency than the unblended coals. This can be explained by the fact that biomass introduces elements that are more probable to enter the gas phase and at the same time combine with the ash elements of the coal ash, therefore the total available solids for deposition is becoming less. This is however common observation in cofiring coals with biomass.

4.7 XRD analyses

4.7.1 Literature review on X-ray diffractometry

In addition to the ICP analyses, the deposit and filter ash samples were submitted to X-ray diffractometry (XRD) which is one of the most common and widely used methods (together with SEM) for the identification and characterization of mineral matter in fly ash. The advantage of this technique is the detection of occurrence and degree of crystallinity of forming major, and some minor crystalline phases (quartz, mullite, magnetite, hematite, feldspars, anhydrite, clay minerals, calcite, cristobalite, and others) independent from their size. This is an advantage for the finely dispersed fly ashes. Individual mineral grains separated from fly ashes can be analyzed. Furthermore, some information for the non - crystalline or poorly crystallized phases can also be obtained.

In [71] the mineral transformations and ash formation during O_2/CO_2 combustion of four pulverized Chinese coals were studied. The coals were combusted in a drop tube furnace to generate ash under various combustion conditions. The ash samples were characterized with XRD analysis and Fe Mössbauer spectroscopy. The impacts of O_2/CO_2 combustion on mineral transformation and ash formation were explored through comparisons between O_2/CO_2 combustion and O_2/N_2 combustion. It was found that, O_2/CO_2 combustion did not significantly change the mineral phases formed in the residue ashes, but did affect the relative amounts of the mineral phases. In [72] an in situ high-temperature X-ray diffraction study of phase transformations in pyrite under variable environmental conditions (atmospheric pressure (1 atm.), low air pressure (<0.001 atm.), inert and carbon dioxide atmosphere) is presented, for oil shale and coal combustion, fuels with considerable amount of pyrite which undergoes various thermal transformations during their processing or combustion. Reactions and changes in pyrite chemistry vary considerably under different environmental conditions. It was observed that while heating of pyrite in air promotes the formation of hematite ([alpha]-Fe_2O_3), magnetite (Fe_3O_4) is a major product in low pressure environment. On the other hand, in the inert environments (nitrogen and argon) pyrrhotite, a non-stoichiometric iron sulphide is the most dominant product. However, in carbon dioxide (CO_2) environment, pyrrhotite is an intermediate low temperature product which further transforms into magnetite and hematite, attributed to the dissociation of the CO_2 into O_2 and CO providing conducive conditions for the oxidation.

Furthermore, several papers stress the importance of Fe mineral transformations. In [73] the chemical speciation of iron in combustion-derived ash is an important factor in determining the likelihood of ash deposit formation and build-up. In [74] the impact of the O_2/CO_2 combustion of a high-aluminum coal was studied, regarding the mineral transformation and fine ash formation in a drop tube furnace. The collected ash samples were characterized in details to study the ash formation behaviours, and the comparison was made between O_2/CO_2 combustion and air combustion. It was found that boehmite transformed to θ-Al_2O_3 and then to α-Al_2O_3 and the extent of the transformation depended upon the residence time and more significantly upon the particle combustion temperature. In comparison to air combustion, O_2/CO_2 combustion did not affect the species of mineral phases formed in the ashes of the coal studied but did affect the relative amounts of the phases. O_2/CO_2 combustion had an impact on the coal par-

ticle combustion temperature and consequently on the ash mineral composition. O_2/CO_2 combustion decreased the yields of the fine ash particles in both the submicrometer fume region and fine fragmentation region as compared to air combustion with the same O_2 concentration because of the decrease in the particle combustion temperature, while an increasing O_2 concentration enhanced the formation of both region particles. The submicrometer particle size formed in O_2/CO_2 combustion was found shifting to a smaller size when compared to that in air combustion.

4.7.2 XRD analysis of samples

Table 4.2 shows the samples submitted to mineralogical analysis. The measurements took place at room temperature in a range of 10-70° 2-theta. The expected mineral phases are shown on Table 4.3.

Table 4.2 *List of samples vs conditions submitted to mineralogical analysis*

Test case	Environment	Ash collected in sensor (g)	Ash collected in filter (g)	Sample ID
1	Lignite (air)		0.7059	f 1
		0.672		s 2
2	Lignite (oxyfuel)		0.2835	f 3
		0.827		s 4
3	Russian coal (air)		0.4983	f 5
		0.281		s 6
4	Russian coal (oxyfuel)		0.2266	f 7
		0.380		s 8
Lignite				c 9
Russian coal				c 10

Table 4.3 *Mineral phases expected in the coals and ash samples*

Ash samples	Coal ash
Quartz (SiO_2)	Quartz (SiO_2)
Mullite ($A1_6Si_2O_{13}$)	Anorthite, ordered ($CaAl_2Si_2O_8$)
Anorthite, ordered ($CaAl_2Si_2O_8$)	Kaolinite ($Al_2SiO_5(OH)_4$)
Calcite ($CaCO_3$)	Calcite ($CaCO_3$)
Anhydrite ($CaSO_4$)	Bassanite ($CaSO_4.0.5H_2O$)
Lime (CaO)	Clinochlore 1MIIb($(Mg,Al,Fe)_6(Si,Al)_4\ O_{10}(OH)_8$)
Pyrrhotite without O_2 ($Fe_{1-x}S$)	Pyrite (FeS_2)
Pyrite (FeS_2)	Hematite (Fe_2O_3)
Hematite (Fe_2O_3)	Siderite ($FeCO_3$)
Magnetite ($Fe^{2+}Fe^{3+}O_4$ or Fe_3O_4)	Dolomite ($CaMg(CO_3)_2$)
Magnesite ($MgCO_3$)	Magnetite ($(Fe_2Fe_{2+3})O_4$ or Fe_3O_4)
Portlandite ($Ca(OH)_2$)	

Finally, the intensity of crystalline and glass phases was compared among the samples, with emphasis in the possible differentiations between air and enriched air/oxyfuel conditions. The results are shown overall in Tables 4.4 and 4.5.

Note: All the samples needed a long measurement time because of the moderate crystalline structure and the minimum presence of most of the minerals, just as already expected.

It is unfortunately not obvious from the results whether there is a considerable difference in the phases formed between air and oxyfuel combustions. The only certain observation is that in some cases the sensor ash phase composition shows differentiation from the filter ash phase composition.

Table 4.4 *XRD results of the ash samples*

	PDF no	f1	s2	f3	s4	f5	s6	f7	s8
quartz	46-1045	x	x	x	x	x	x	x	x
mullite	84-1205	x	x	x	x	x	x	x	x
lime	37-1497	x	x	x	?	x	x	x	x
hematite	89-0599	-	x	-	x	-	x	-	x
anhydrite	72-0916	-	x	-	?	-	-	-	-
magnetite	19-0629	-	?	-	?	-	?	-	?
pyrite	42-1340	-	-	-	?	-	-	-	-
pyrrhotite	71-0647	-	-	-	-	-	-	-	-
calcite	72-1937	-	-	-	-	-	-	-	-
anorthite	41-1486	-	-	-	-	-	-	-	-
magnesite	86-2344	-	-	-	-	-	-	-	-
portlandite	44-1481	-	-	-	-	-	-	-	-

f1=filter ash Lignite (air), s2 = sensor ash Lignite (air), f3=filter ash Lignite (oxy), s4 = sensor ash Lignite (oxy), f5=filter ash Russian coal (air), s6 = sensor ash RC (air), f7=filter ash Russian coal (oxy), s8 = sensor ash RC (oxy)

Table 4.5 *XRD results of the coal ash samples*

	PDF no	c9 = lignite	c10 = Russian Coal
quartz	46-1045	x	x
anorthite, ordered	41-1486	x	?
kaolinite	89-6538 (=2M) 74-1784 (=1A)	x (type 2M)	x (type 1A)
siderite	83-1764	x	x
bassanite	41-0224	x	-
clinochlore 1MIIb	46-1323	x	-
hematite	89-0599	-	-
magnetite	89-0951	x	-
dolomite	75-1759	-	x
calcite	72-1937	-	?
pyrite	42-1340	-	-

The results summary in Table 4.4 show that the main mineral matters in the Lignite is quartz, anorthite, kaolinite type 2M, siderite, bassanite, clinoclore and magnetite while in the Russian coal ash there is quartz, probably anorthite, kaolinite type 1A, siderite, dolomite, magnetite and likely calcite

In Figures 4.7 – 4.10 the XRD patterns of the deposit and filter ash samples are shown, while in Figures 4.11 and 4.12 the diffractograms of the 800^{o}C ashed Lignite and Russian coal samples are shown as reference.

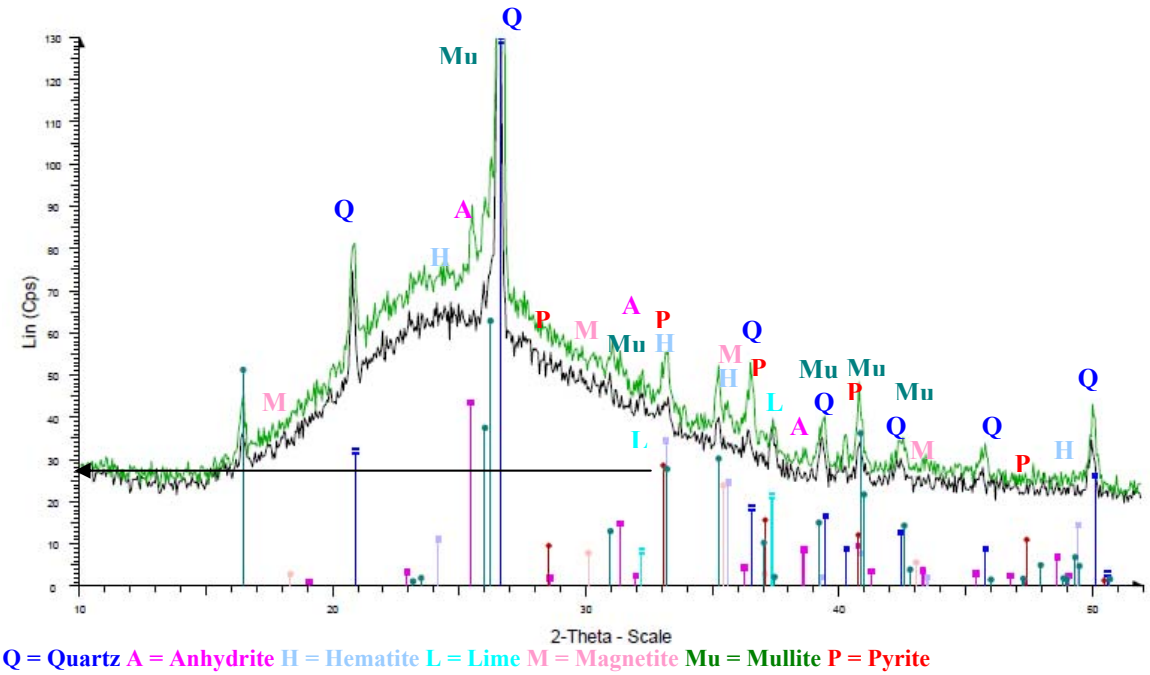

Figure 4.7 *Fly ash (f1 – black line) and deposited ash (s2 – green line) from Lignite under air combustion*

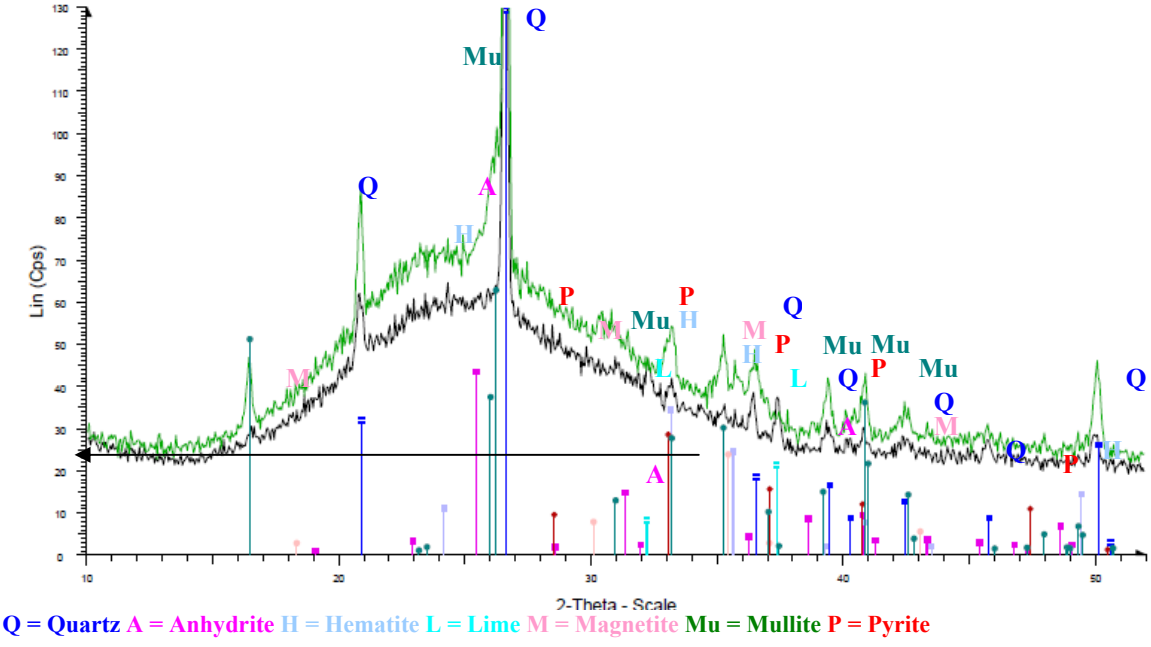

Figure 4.8 *Fly ash (f3 – black line) and deposited ash (s4 – green line) from Lignite under oxyfuel combustion*

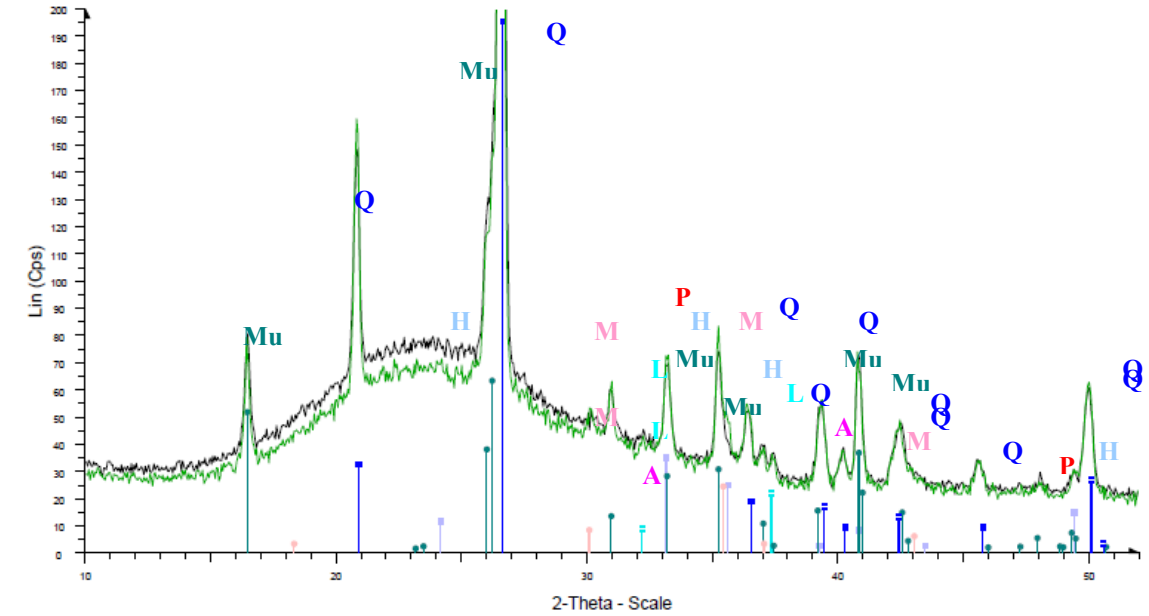

Figure 4.9 *Fly ash (f5 – black line) and deposited ash (s6 – green line) from Russian coal under air combustion*

No Pyrite and Anhydrite was detected in Figure 6.4.

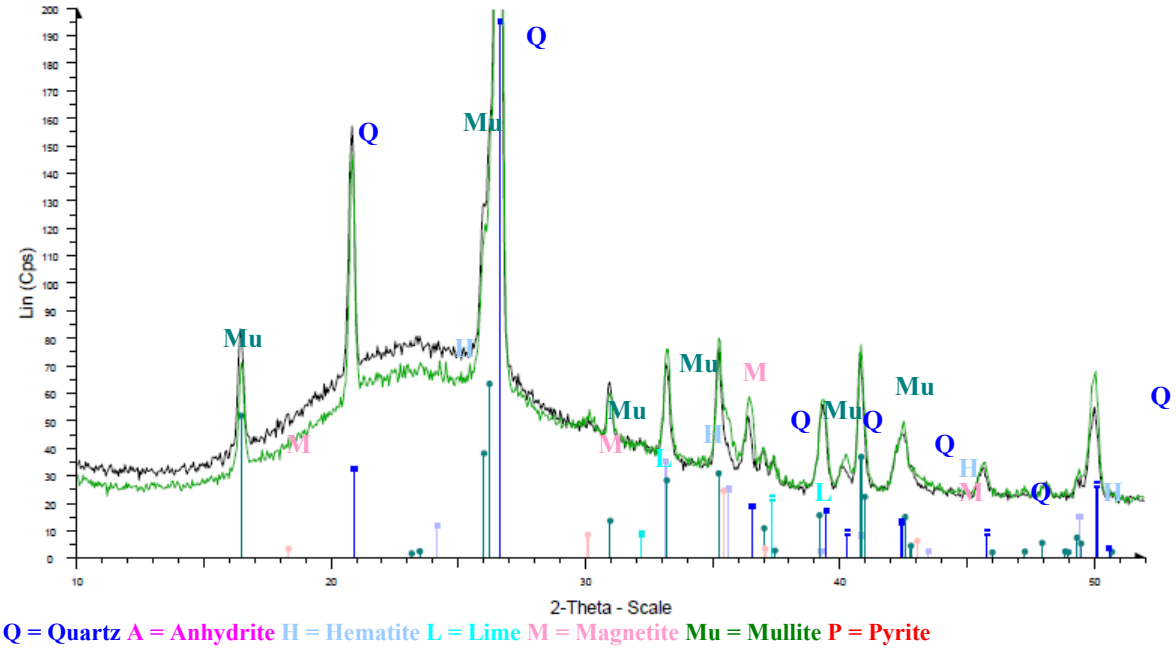

Figure 4.10 *Fly ash (f7 – black line) and deposited ash (s8 – green line) from Russian coal under oxyfuel combustion*

No Pyrite and Anhydrite was detected in Figure 4.10

At a first glance there does not seem to be a considerable variation among the mineral phases of the samples under the various combustion conditions. Moreover, some amount of glass phase was detected, and this is also probably the reason for the lack of precision in the results, with the peaks overlapping.

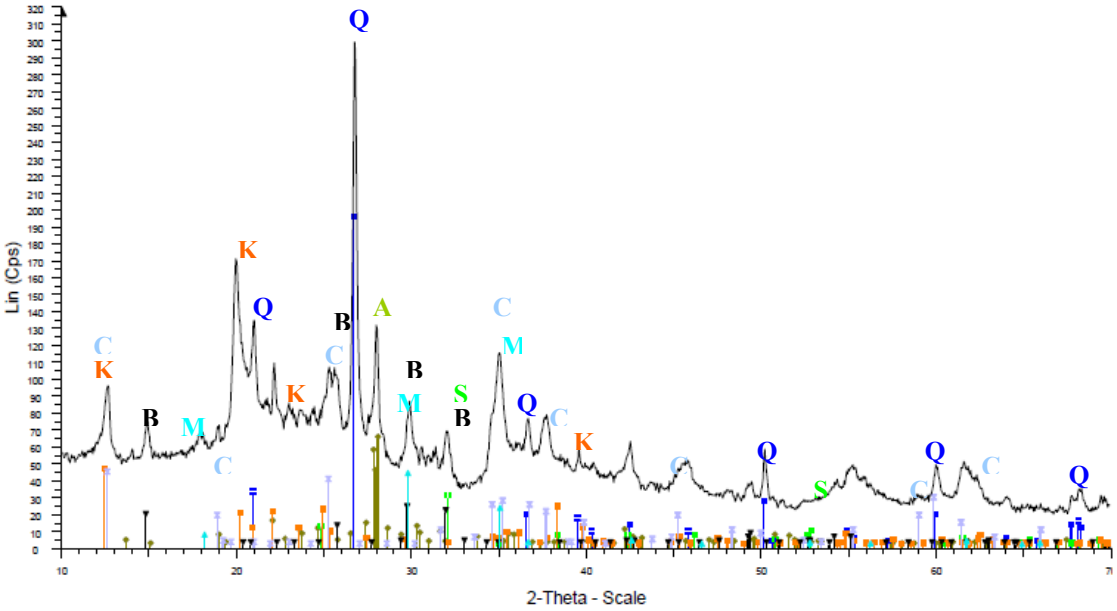

Figure 4.11 *Lignite coal ash diffractogram*

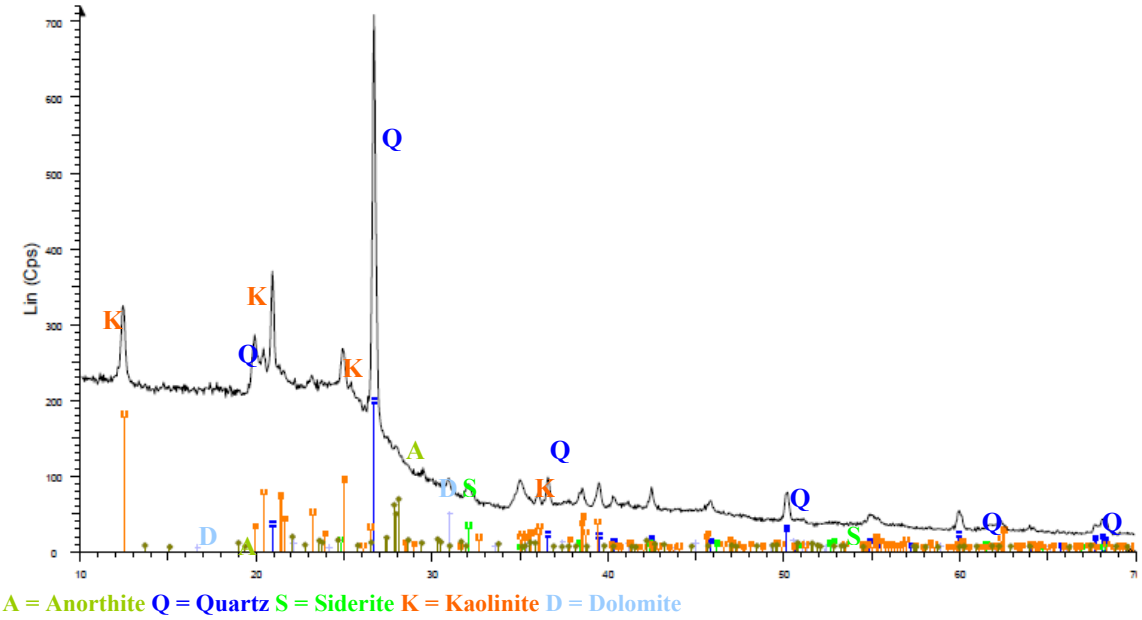

Figure 4.12 *Russian coal ash diffractogram*

4.7.3 Evaluation of the phase transformation results

The major conclusion is that in the current presented tests no variations in the phases were observed between air and oxyfuel tests. The intensity of the signals was just the

same in both cases. Of course variations were observed among the ash samples, however these variations are not due to the combustion environment, but simply due to the different fuel origin. A few comments on the phase transformations will be given here.

For the case of lignite, quartz (SiO_2) remains in the ash in both cases. Anorthite (Ca-Al-Si) and kaolinite (Si-Al) is probably transforming to Mullite (Si-Al) and Quartz, while the Ca content is found in Lime (CaO), Anhydrite ($CaSO_4$). However Anhydrite could be the direct water removal from the phase Bassanite ($CaSO_4.0.5H_2O$). In Lignite, Bassanite is also the only phase that contains the element of S. Fe is contained in the phases of Siderite ($FeCO_3$), Clinochlore (Mg-Al-Fe-Si-Al) and mainly Magnetite (Fe_3O_4). Magnetite is also found in the ashes of both combustion conditions, but the elements mainly recombine into hematite (Fe_2O_3) and the stable Pyrite (Fe_2S).

For the case of Russian coal, quartz (SiO_2) remains in the ash in both cases. Anorthite (Ca-Al-Si) and kaolinite (Si-Al) is probably transforming to Mullite (Si-Al) and Quartz, while the Ca content initially bound in Dolomite ($CaMg(CO_2)_3$), Anorthite and kaolinite are transformed into Lime (CaO). Fe is contained in the phase of Siderite ($FeCO_3$). This is probably transforming into magnetite and hematite (Fe_2O_3). However it is remarkable that S was not present in any phase neither in the coal ash neither in the produced ash in the form of pyrite (FeS_2) for example. It could justifie that no S is found in the residual ash, as it was also not detected with the ICP, however there is S in the raw coal, therefore phases including S were expected. For this reason, a further XRD measurement series will take place in the near future.

Another remark is that Hematite (Fe_2O_3) was only present in the sensor ash samples and not at all in the fly ash. The same goes for Anhydrite ($CaSO_4$), it was only present in the sensor ash and only in the Lignite case. Magnetite was present in very small amounts in the sensor ashes, while as mentioned the signal of pyrite was very weak and only present in the sensor ash of the oxyfuel case for Lignite.

The absence of carbonates in the oxyfuel ashes ($CaCO_3$, $MgCO_3$, $FeCO_3$) indicates that no carbonation took place despite the large CO_2 concentrations. This should be investigated further by performing long term tests, possibly also corrosion tests, in order to establish possible corroding impact of high CO_2 concentration on both corrosion of metallic surfaces as well as promoting higher deposition due to carbonation of elements.

4.8 Chemical equilibrium calculations

4.8.1 The use of FACTSage® 5.5

In order to assist the interpretation of the experimental results, chemical equilibrium calculations were performed using the equilibrium module and the integrated database of the computer program FACTSage® 5.5, using as input the fuel analyses of the first test series (Russian and South African coal and cocoa blends). FACTSage® calculates the concentrations of chemical species when specified elements or compounds react or partially react to reach a state of chemical equilibrium. The calculations are performed by minimization of the Gibbs free energy from the system subjected to mass balance constraints. This approach provides a first useful description of ash reactions in complex systems. However, it assumes infinitely fast reactions and therefore, it is not sufficient to describe transient processes. The compounds and phases predicted in these calculations are the more stable products (thermodynamically controlled products) and kinetic limitations are not taken into account. Moreover, the temperature his-

tory of the fuel particles during the combustion process is not taken into account and the calculations of the final product at each temperature are done independently considering always the average elemental fuel composition as the reactants and assuming perfect mixing. Therefore it has to be noted that differences in the ash formation under air or oxy conditions due to theses differences in the process will not be reflected in the products predicted by chemical equilibrium calculations.

4.8.2 Scope of work and description of settings

The reactants are introduced in elements as obtained from the ultimate (C, S, O, H, and N) and the elemental analyses of the fuel (Al, Ca, Fe, K, K, Mg, Na, P, Si and Cl), in grams of the elements contained in 1 kg of dry fuel. Trace elements have not been included in these calculations. The oxidant input corresponding to an air ratio 1.2 is also included in the reactants, being O_2 and N_2 (with a mixing ratio equal to that in air, i.e. 21 vol. % of O_2) for the air combustion and O_2 and CO_2 for the oxyfuel combustion (with a mixing ratio of 30 vol. % of O_2).

The calculations are performed for a temperature range between 800 – 1800^{o}C and atmospheric pressure. The possible products selected are the entire compound species (ideal gases, pure solids and pure liquids) from the ELEM, FToxid, FTsalt and FACT53 databases and the solutions species selected are listed in Table 5.3. When the same compound is included in more than one database, only those compounds from one database have been selected with attention to the priority list: ELEM, FToxid, FTsalt and FACT53. The slag model chosen in the FACTSage® calculations was the BSlag-liquid. This model includes oxide components (oxides of Al, Si, Fe, Mg, Ca, Na and K) in solutions with SO_4. FACTSage® has, among other slag models, the slag model FToxid-SLAG?, which allows to include the oxides and all non oxide components (F, Cl, S, SO_4, PO_4, CO_3, OH/H_2O) melting together in the slag phase. However, due to its complexity, the use of this model is not encouraged, as it is not optimized for many solutions and the selection of input must be very specific. Models ASlag-liquid and CSlag-liquid have also been tried, but the differences found were minor, apart from the fact that their databases are not as suitable for the present chemical system.

Table 4.6 *Solution species included in the Factsage calculations*

Database	**Phase (Full Name)**	**Phases***
Liquid solutions		
FToxid	SLAGB (BSlag-liq)	2
FTsalt	SALTF (FSalt-liquid)	3
Solid solutions		
FToxid		
	SPIN (Spinel)	2
	MeO_A (AMonoxide)	1
	cPyr (Clinopyroxene)	1
	oPyr (Orthopyroxene)	1
	pPyr (Protopyroxene)	1
	LcPy (LowClinopyroxene)	1
	WOLLA (AWollastonite)	1
	aC2SAAa (Ca_2SiO_4)	1
	Mel_ (Melilite)	1
	Oliv (Olivine)	2
	Cord (Cordierite)	1
	CORU (Corundum)	2
	NCSO ($Na_4CaSi_3O_9$ – $Na_2Ca_2Si_3O_9$ solid solution)	1
FTsalt		
	ACL_B (BAlkCl-ss_rocksalt)	3
	ALOH (K, Rb, Cs, [Na]//OH(HT)	1
	AOH_ (KOH-RbOH-[NaOH](LT)	1
	KCO_ (K,Na//CO_3,SO_4(ss))	2

KCOH (KCl-KOH(ss))	1
KNSO ($K3Na(SO_4)_2$)	1
KSO_(K,Na//SO_4,CO_3(ss))	2
NCOA (NaOH-[NaCl](ss))	1
NCOB (NaCl-[NaOH](ss))	1
NKCA (Na_2CO_3-[K_2CO_3](LT))	1
NKCB (Na_2SO_4-[K_2SO_4](ss))	1
NKSO (Na2SO4-[K2SO4](ss))	1
SCSO (K, [Ca]//CO_3,SO_4(ss))	2
SSUL (Na,[Mg,Ca]//SO_4(ss))	1

*1: single phase 2: possible 2-phase immiscibility 3: possible 3-phase immiscibility

4.8.3 Results and discussion

In the following paragraphs, the presentation of the equilibrium results is directly linked to the chemical analysis results and the observations on the deposition behavior presented in the previous paragraphs.

Figure 4.12 shows the maximum slag and solid ash formed for 1000 gr of dry fuel input, according to chemical equilibrium calculation results, for the combustion of the two coals in O_2/CO_2 and air and their blends with Cocoa (20 % wt.). The results seem almost identical for air and oxyfuel. Higher amounts of slag and solid phases are predicted for the pure coals compared to their blends with cocoa. The higher amounts of solid phase predicted in the pure fuels' cases are in line with the observed ash deposition behavior, where a somewhat higher deposition behavior was observed for the pure fuels' test cases. The increased input of Cl in the blend through cocoa most probably contributes to elements volatilization, reducing their tendency to form solid compounds that deposit. Other researchers have reported the formation of simple alkali salts (KCl, K_2CO_3, Na_2SO_4 and K_2SO_4) in the melted phase of biomass ashes [75, 76] for fluidized bed combustors. In our case, no salt liquid solution (KCl, K_2CO_3, Na_2SO_4 and $K_2SO_4)_{(liq)}$ has been obtained for the considered chemical system, which is in line with the SEM/EDS observations and ICP results of the deposit samples that did not show S and Cl in the deposited and filter ash. The oxides in the slag solution are the same predicted in the solid phase. The total sum of the amounts of the solid and the slag phase are constant, and what is changing is their relative percentage while temperature increases.

As mentioned, the ash samples collected in the deposition probes at the end of the experiments were loose and powdery. Nevertheless, during the combustion process the fuel particles are exposed to temperatures reaching the melting point of some of the ash forming compounds. In addition, vaporization and condensation of these compounds can occur. The rounded shape of some particles observed in the microscope supports the argument of particles' softening, not leading to slag formation though, as predicted by FACTSage®. Predictions on chemical equilibrium of solid compounds based on FACTSage® should be evaluated considering a number of parameters that affect ash formation mechanisms and slag formation but are not considered by the specific software. Examples of theses parameters are the coal rank, fuel mineral matter composition, the initial particle size distribution of the fuel, agglomeration of ash particles with melted ash, the slag film build up on heat transfer surfaces, the particles residence time, the type of combustion system (air staging or not), heating rate of the particles.

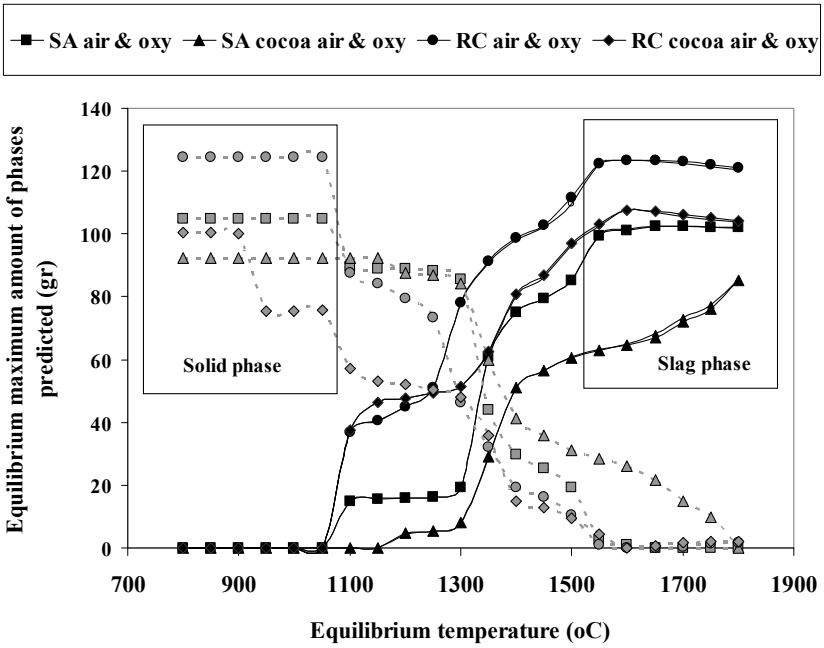

Figure 4.13 *Equilibrium amount (in gr / 1000 gr dry fuel) of the slag and solid phase predicted by FactSage® versus temperature for the two coals and their blends under air and oxyfuel combustion conditions*

In specific, special attention must be paid when analyzing FACTSage® quantitative estimations of the amount of slag formed, especially concerning the potassium. The calculations do not take into account the reactivity of potassium, which varies considerably between coals and biomass fuels. The K bound in coal ash is more inert (forming alumino- silicates), than the K found in the biomass ash, which is generally not bound in silicates. The reactivity of K affects the dominating K compounds finally formed and therefore when K_2O is present in the slag model the results are much less reliable.

Among the generally accepted as volatile inorganic elements (S, K, Cl), that affect the ash formation and deposition behaviour, K was chosen to be studied in more detail, as S and Cl are predicted to convert into the gaseous compounds up to 100%. Figure 4.13 shows the percentage of fuel – K found in the gas phase for all the fuels and blends. The following discussion includes comments on the fate of K, S and Cl.

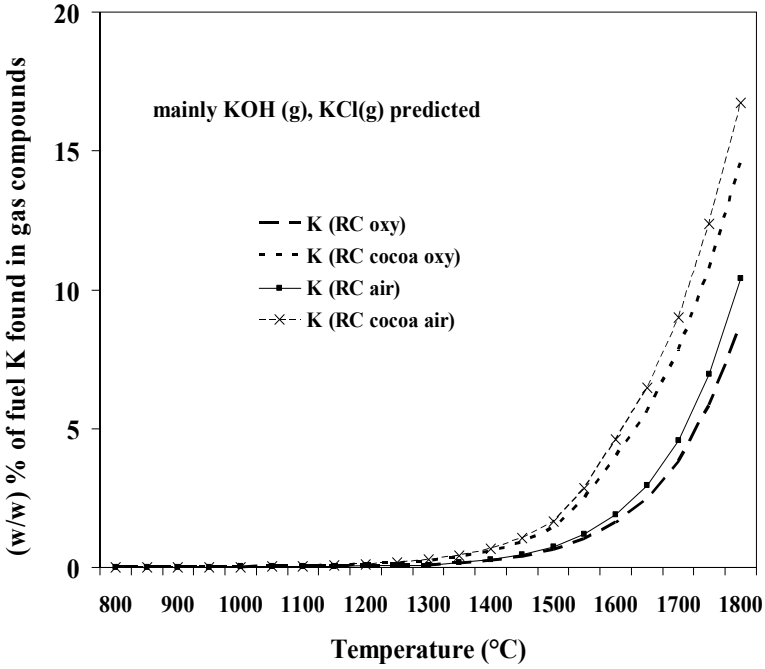

(a) Russian Coal & blends

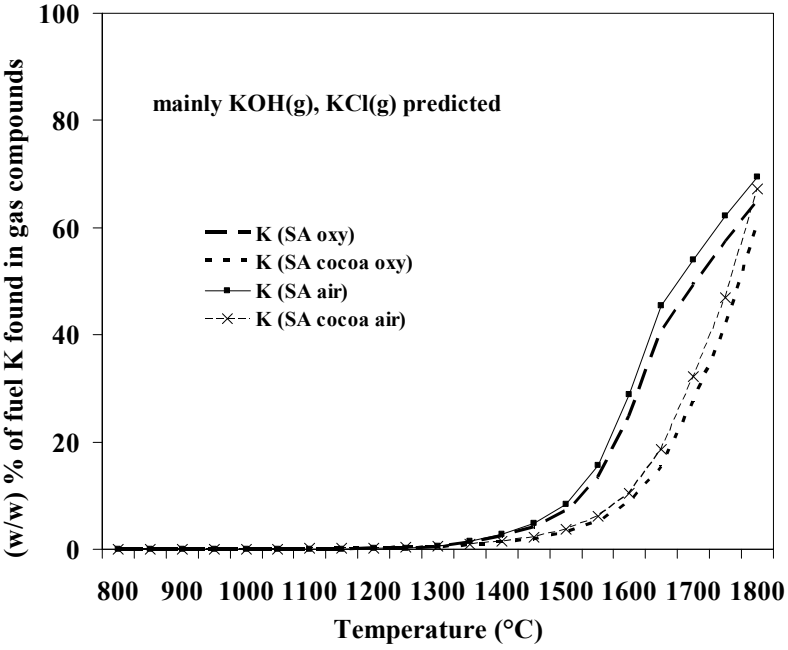

(b) South African Coal & blends

Figure 4.14 *Weight percentage (% w/w) of the fuel - K found in gas compounds calculated with FactSage®*

A major percentage of the fuel-K forms potassium aluminum silicate (solid phase) or is found in the slag phase in the form of oxides, according to FACTSage® calculations. For the unblended coals in air and oxyfuel the major part of the Cl forms HCl, which unlike alkali chlorides does not condense and therefore Cl is not expected in the deposit, as verified during the ash analyses. The gaseous percentage of K is small both for the unblended coal and the blend case due to the fact that most of the alkalis are

bound in aluminum silicates forming $KAlSi_2O_6$, $NaAlSi_3O_8$ and $KAlSi_3O_8$ (leucite and feldspars). This explains the presence of K in the deposited ash as well as in the fine ash. Aho and Ferrer [77] suggested that this mechanism in the co-firing of coal and biomass prevents chlorine deposition. Similar chemical equilibrium results were obtained by Wei et al. [78] for the co-combustion of coal and straw.

In detail, for the Russian coal in air and oxyfuel, fuel K in the gas phase is found mainly as $KOH_{(g)}$ and to a lesser extent $KCl_{(g)}$, under both conditions. For Cl the tendency is to form $HCl_{(g)}$, and at higher temperatures some $KCl_{(g)}$ starts to appear, with a maximum mass concentration of 15%. The $KCl_{(g)}$ released is slightly higher under air combustion, what is in accordance with the higher K-enrichment in the submicron particle range observed in the experiments. These two compounds together constitute almost 100% of the Cl species, all in the gas phase, with some elemental Cl formation predicted as well. S is all released to the gas phase, converted mainly to SO_2, and to a lesser extent to SO_3. At high temperatures, almost no SO_3 is found, and SO_2 is the thermodynamically favourable compound.

For the Russian coal/cocoa blends under both air and oxyfuel, the trend is the same for the fuel - K distribution. Elemental K is also found, as well as a small percentage of $K_2SO_{4(g)}$. S and Cl are released in the gas phase up to 100%. HCl is formed in percentages ranging from 100% for the low temperatures down to ~ 20% for very high temperatures, while $KCl_{(g)}$ follows the opposite trend, starting at 0% and reaching ~ 25% of the fuel K converted into $KCl_{(g)}$. For S the trend is also the same as previously described, mostly SO_2 is formed, especially at high temperatures, while at low temperatures a small percentage of fuel - S to SO_3 was predicted as well. However, due to the Ca present in the ash, some $CaSO_4$ is predicted as a solid phase.

For the South African coal under oxyfuel and air, K shows the same trend as in the Russian coal case. The tendency is the same for Cl and S as well. In the South African/cocoa blends under oxyfuel and air combustion, again the same tendency was observed as in the Russian coal blend with cocoa, for K, Cl and S.

4.8.4 Conclusions and remarks

Focusing on the tendencies of the elements shown in Figures 4.12 and 4.13, and their link with the experimental results, it is suggested that the K findings are generally in line with the experimental data. K is found back mostly in the deposited and filter ash, as the enrichment factor reveals (*EF* =1) while S and Cl are almost completely absent from the ash. The small $KCl_{(g)}$ amount predicted by the equilibrium calculations is expected to condense forming submicron particles, as observed in the cascade impactor experiments that showed Na, K and Cl enrichment in the finer ash.

Comparing the results for the coals and coal/cocoa blends, it can be remarked that a higher amount of gaseous compounds was released in the case of the blends. The reason probably is the Cl content of the ash, which is higher in the blends and facilitates the volatilization of elements, especially K. Furthermore, in the case of South African coal and its blends the gaseous release is even higher. In that case, this could be attributed to the generally higher Cl/K ratio that contributes to a larger extent to the volatilisation of the available K, as shown in the fuels analysis Table. A last comment is that the somewhat different flame temperatures during air and oxy-combustion do not justify a large variation in the predicted solid/slag/gas phases.

5. General conclusions

The observed ash composition, ash formation and ash deposition behaviour of the coals and blends under air and oxyfuel conditions showed some variations. In specific, the fouling factor (the resistance to heat transfer) was higher for the oxyfuel cases, while the deposition propensities were also higher for the coals under oxyfuel conditions. Based on these observations, it has been attempted to analyse the parameters that affect the ash formation and deposition behaviour of fuels and filter out the parameters related to the particular case of oxyfuel combustion, in an attempt to explain the observed results. First, particle size distribution differences were observed, in numerous cases the particle size was shifted to increased areas in the oxyfuel case. The reason for this can be locally increased char combustion temperatures that can lead to local melt formation, ash droplet formation and agglomeration of small particles. However not all samples analysed confirmed this tendency. Further on, the carbon in ash was measured but no unburnt char increase was observed in the oxyfuel case that could artificially increase the deposited ash. The crystallographic composition of the ashes could not indicate some strong variations in the phases formed (e.g. iron containing phases or carbonates) that would explain a serious deposition behaviour deviation in the two conditions. The elemental ash composition given from the ICP analyses did not show differences related to the combustion environment. In a previous work we observed variations in the refractory elements of the fine ash particles (micron and submicron) but not the bulk ash composition. Therefore, due to all the above observations, we conclude that we have to search further the causes of this varying deposition pattern. The flue gas properties between air combustion and oxyfuel combustion are different, as the CO_2 is denser and has different viscous/elastic behaviour. This leads probably to changes in the flow field (velocities, particle trajectory) that causes the observed effects. The combined effect of all the above mentioned parameter sis finally expected to be the answer of the observed results. For example, particle size distribution continues to play a significant role, as very small particles will not easily impact the surfaces, because they will be carried away by the gas flow. For the same gas (same viscous behaviour), and for the same gas velocity, larger particles are more prone to impact on the surfaces, as they will not follow the flow field around the deposition tube (deposition surface). However of the gas changes, then ash with the same particle size will behave different in a more viscous flow. Therefore it was decided to study the influence of fluid dynamic characteristics (gas composition, temperature, velocities) and ash particle related characteristics (particle sizes, composition & density) under various operating conditions, which is presented in Part II.

The conclusions drawn at lab scale need to be considered carefully when applying at full scale. The LCS is a down-fired entrained-flow drop-tube-like test rig, in which all the particles, independent of the size and composition will end up at the bottom, where the sampling train is located, and in the filter ash. In a full-scale power plant, opposed-, tangentially or down-fired, the prevailing deposition mechanisms are more complicated, affecting the ash distribution. However, the conclusion that under oxyfuel conditions systematically less fine ash was found back in the filter (fly ash) and more coarse ash

was deposited, as opposed to the air case, can prove useful in the design of the heat exchanger tubes and surfaces generally, preventing excessive fouling in points that were not considered under conventional air operation. More information is necessary in order to make clear practical conclusions, gained from testing different fuels that will produce various particle size distributions of ash and simulations of ash deposition using CFD (computational fluid dynamics) in order to evaluate the observed results and point out.

References

[1] International Energy Agency (IEA) Bioenergy Task 40: 'Sustainable International BioEnergy Trade: Securing supply and demand'. Co-firing Report- United Kingdom: The Bioenergy Group (BEG) Imperial College London, Centre for Energy Policy and Technology (ICEPT), Miles Perry & Frank Rosillo-Calle Report T40UK02R, November 2006

[2] IPCC Special Report on Carbon Dioxide Capture and Storage

[3] B.J.P. Buhre, L.K. Elliott, C.D. Sheng, R.P. Gupta, T.F. Wall Oxy-fuel combustion technology for coal-fired power generation, Progress in Energy and Combustion Science 31 (2005)

[4] Singh D, Croiset E, Douglas PL, Douglas MA. Techno-economic study of CO_2 capture from an existing coal-fired power plant: MEA scrubbing vs. O_2/CO_2 recycle combustion. Energy Conversion and Management, 2003; 44:3073–91.

[5] Tan Y, Douglas M., Thambimuthu K., CO_2 capture using oxygen enhanced combustion strategies for natural gas power plants. Fuel 2002; 81:1007–16.

[6] Department Of Energy, Fossil Energy, Enhanced Oil Recovery/CO_2 Injection (http://www.fossil.energy.gov/programs/oilgas/eor/index.html)

[7] http://www.co2sequestration.info/co2db.htm , access date: June 2007.

[8] Kiga T, Takano S, Kimura N, Omata K, Okawa M, Mori T, et al., Characteristics of pulverised-coal combustion in the system of oxygen/recycled flue gas combustion. Energy Conversion and Management, 1997; 38:S129–S34.

[9] Várhegyi G, Till F. Comparison of temperature-programmed char combustion in CO2–O2 and Ar–O2 mixtures at elevated pressure. Energy Fuels 1999;13:539–40.

[10] Varheyi G, Szabo P, Jakab E, Till F. Mathematical modeling of char reactivity in Ar–O2 and CO2–O2 mixtures. Energy Fuels 1996;10:1208–14.

[11] Okazaki K, Ando T. NO_x reduction mechanism in coal combustion with recycled CO2. Energy 1997; 22:207–15.

[12] Hu YQ, Kobayashi N, Hasatani M. Effects of coal properties on recycled-NO_x reduction in coal combustion with O2/recycled flue gas. Energy Conversion and Management

[13] Hu Y, Naito S, Kobayashi N, Hasatani M. CO2, NOx, and SO2 emissions from the combustion of coal with high oxygen concentration gases. Fuel 2000;79:1925–32.

[14] Hu YQ, Kobayashi N, Hasatani M. The reduction of recycled-NO_x in coal combustion with O_2/recycled flue gas under low recycling ratio. Fuel 2001, 80:1851–5.

[15] Liu H, Katagiri S, Kaneko U, Okazaki K. Sulfation behaviour of limestone under high CO2 concentration in O2/CO2 coal combustion. Fuel 2000;79:945–53.

[16] Liu H, Kagajo T, Kaneko U, Okazaki K. Drastic SOx removal and influences of various factors in O2/CO2 pulverized coal combustion system. Energy Fuels 20,01;15:403–12.

[17] Krishnamoorthy G, Veranth JM. Computational modeling of CO/CO2 ratio inside single char particles during pulverized coal combustion. Energy Fuels 2003;17:1367–71.

[18] Zheng L, Furimsky E. Assessment of coal combustion in O2/ CO2 by equilibrium calculations. Fuel Process Technol 2003;81: 23–34.
[19] Emission Characteristics of the 0.03 MW Oxy-Fuel Combustor, Ho Keun Kim and Yongmo Kim, Energy & Fuels 2006, 20, 2125-2130
[20] Soot and NO formation in methane–oxygen enriched diffusion flames *Combustion and Flame*, *Volume 124, Issues 1-2*, *January 2001*, *Pages 295-310* A. Beltrame, P. Porshnev, W. Merchan-Merchan, A. Saveliev, A. Fridman, L. A. Kennedy, O. Petrova, S. Zhdanok, F. Amouri and O. Charon
[21] Studies on Combustion Characteristics and Flame Length of, Turbulent Oxy-Fuel Flames, Ho Keun Kim and Yongmo Kim, American Chemical Society, Published on Web 04/06/2007
[22] Quantitative laser-saturated fluorescence measurements of nitric oxide in counter-flow diffusion flames under sooting oxy-fuel conditions, Combustion and Flame, Volume 129, Issues 1-2, April 2002, Pages 112-119, Sameer V. Naik and Normand M. Laurendeau
[23] Simultaneous easy CO2 recovery and drastic reduction of Sox and NOx in O2/CO2 coal combustion with heat recirculation, Fuel 82 (2003) 1427–1436
[24] Low NOx combustion technologies for high temperature applications, Energy Conversion and Management, Volume 42, Issues 15-17, Pages 1919-1935 Michael Flamme
[25] A laboratory study on the NO, NO2, SO2, CO and CO2 emissions from the combustion of pulverized coal, municipal waste plastics and tires, Fuel, Vol. 77, No. 3. pp. 183-196. 1998
[26] Journal of Hazardous Materials 142 (2007) 266–271, Emission characteristics of coal combustion in different O2/N2, O2/CO2 and O2/RFG atmosphere, Jyh-Cherng Chen, Zhen-Shu Liu, Jian-Sheng Huang
[27] Combustion and Flame 144 (2006) 710–729, Combustion kinetics of coal chars in oxygen-enriched environments, Jeffrey J. Murphy 1, Christopher R. Shaddix
[28] Fuel conversion from oxy-fuel combustion in a circulating fluidized bed, T. Czakiert, Z. Bis, W. Muskala, W. Nowak, Fuel Processing Technology 87 (2006). 531–538
[29] Pulverized coal combustion in air and in O2/CO2 mixtures with NOx recycle
Hao Liu, Ramlan Zailani, Bernard M. Gibbs, Fuel 84 (2005) 2109–2115
[30] Study report, IFRF Doc. No G23/y/1. Oxy coal Combustion with flue gas recycle for the power generation industry – A literature review.
[31] Combustion of pulverized coal using waste carbon dioxide and oxygen, Combustion and Flame, Volume 72, Issue 3, June 1988, Pages 301-310, C. S. Wang, G. F. Berry, K. C. Chang and A. M. Wolsky
[32] Woycenko D., van de Kamp W., Roberts P., Combustion of pulverized coal in a mixture of oxygen and recycled flue gas, in summary of the APG research program 1995 [JOU2-CT92-0093, IFRF Doc F98/Y/4].
[33] Kimura K, Omata K, Kiga T, Takano S, Shikisima S. Characteristics of pulverized coal combustion in O_2/CO_2 mixtures for CO_2 recovery. Energy Conversion and Management, 1995;36: 805–8.
[34] Nozaki T, Takano S, Kiga T, Omata K, Kimura K. Analysis of the flame formed during oxidation of pulverised coal by an O_2– CO_2 mixture. Energy 1997; 22(2/3): 199–205.
[35] Croiset E, Thambimuthu KV. NO_x and SO_2 emission from O_2/CO_2 recycle coal combustion. Fuel 2001;80:2117–21.
[36] Modeling of oxy-fuel combustion for a western Canadian sub-bituminous coal, Eddy H. Chui, Mark A. Douglas, Yewan Tan, Fuel 82 (2003) 1201–1210
[37] 1st IEA GHG Oxyfuel Conference, Cottbus, 12-15 September 2009.
[38] Numerical investigation of oxy-coal combustion to evaluate burner and combustor design concepts, Energy, Volume 29, Issues 9-10, July-August 2004, Pages 1285-1296, E. H. Chui, A. J. Majeski, M. A. Douglas, Y. Tan and K. V. Thambimuthu

[39] Combustion characteristics of coal in a mixture of oxygen and recycled flue gas, Fuel, Volume 85, Issue 4, March 2006, Pages 507-512, Yewen Tan, Eric Croiset, Mark A. Douglas and Kelly V. Thambimuthu
[40] High efficiency electric power generation: The environmental role, Janos M. Beer, Progress in Energy and Combustion Science 33 (2007) 107–134
[41] Energy 32 (2007) 1163–1176, Performance and costs of power plants with capture and storage of CO2, John Davison
[42] Comparative assessment of sub-critical versus advanced super-critical oxyfuel fired PF boilers with CO2 sequestration facilities, Sina Rezvani, Ye Huang, David McIlveen-Wright, Neil Hewitt, Yaodong Wang, available online in Fuel (2007)
[43] Oxy-combustion processes for CO2 capture from advanced supercritical PF and NGCC power plant, D J Dillon, R S Panesar, R A Wall, R J Allam, V White, J Gibbins & M R Haines, IEA Greenhouse Gas R&D Programme
[44] IEA Greenhouse Gas R&D Program. Potential for Improvements in Gasification Combined Cycle Power Generation with CO2 Capture, IEA Greenhouse Gas R&D Programme Report PH4/19, May 2003 (http://www.ieagreen.org.uk/)
[45] First National Conference on Carbon Sequestration, May 15-17 2001, Washington DC, CO_2 Capture via Oxyfuel Firing: Optimisation of a Retrofit Design Concept for a Refinery Power Station Boiler, Michael B Wilkinson, John C Boden, Raghbir S Panesar, Rodney J Allam
[46] T. Wall, Y. Liu, C. Spero, L. Elliott, S. Khare, R. Rathnam, F. Zeenathal, B. Moghtaderi, B. Buhre, C. Sheng, R. Gupta, T. Yamada, K. Makino, J. Yu, An overview on oxyfuel coal combustion—State of the art research and technology development, Chemical Engineering Research and Design 87 (2009) 1003-1016.
[47] C. Sheng, Y. Li, X. Liu, H. Yao, M. Xu, Ash particle formation during O_2/CO_2 combustion of pulverized coals, Fuel Processing Technology 88 (2007) 1021–1028.
[48] B.J.P. Buhre, L.K. Elliott, C.D. Sheng, R.P. Gupta, T.F. Wall, Oxy-fuel combustion technology for coal-fired power generation, Progress in Energy and Combustion Science 31 (2005) 283-307.
[49] C. Sheng, Y. Lu, X. Gao, H. Yao, Fine ash formation during pulverized coal combustion – A comparison of O_2/CO_2 combustion versus air combustion, Energy & Fuels 21 (2007) 435-440.
[50] C. Sheng, Y. Li, Experimental study of ash formation during pulverized coal combustion in O_2/CO_2 mixtures, Fuel 87 (2008) 1297-1305.
[51] A. Suriyawong, M. Gamble, M.-H. Lee, R. Axelbaum, P. Biswas, Submicrometer particle formation and mercury speciation under oxygen– carbon dioxide coal combustion, Energy Fuels 20 (2006) 2357–2363.
[52] M. Theis, B. J. Skrifvars, M. Zevenhoven, M. Hupa, H. Tran, Fouling tendency of ash resulting from burning mixtures of biofuels, Part 2: Deposit chemistry, Fuel 85 (2006) 1992-2001.
[53] P. F. Nelson, Trace Metal Emissions in Fine Particles from Coal Combustion, Energy & Fuels 21 (2007) 477-484.
[54] P. Bejarano, Y.A. Levendis, Single-coal-particle combustion in O_2/N_2 and O_2/CO_2 environments, Combustion and Flame 153 (2008) 270-287.
[55] J.J. Murphy, R. C.R. Shaddix, Combustion kinetics of coal chars in oxygen-enriched environments, Combustion and Flame 144 (2006) 710–729.
[56] G. Krishnamoorthy, J.M. Veranth, Computational modeling of CO/CO_2 ratio inside single char particles during pulverized coal combustion, Energy Fuels 17 (2003) 1367–1371.
[57] A.R. McLennan, G.W. Bryant, B.R. Stanmore, T. F. Wall, Ash Formation Mechanisms during PF Combustion in Reducing Conditions, Energy & Fuels 14 (2000), 150-159.
[58] L. Zheng, E. Furimsky, Assessment of coal combustion in O_2/CO_2 by equilibrium calculations, Fuel Processing Technology 81 (2003) 23-34.

[59] Y. Zhao, J. Zhang, H. Liu, J. Tian, Y. Li, C. Zheng, Thermodynamic equilibrium study of mineral elements evaporation in O_2/CO_2 recycle combustion, Journal of Fuel Chemistry and Technology 34 (2006) 641-649.
[60] N. Otsuka, A thermodynamic approach on vapor-condensation of corrosive salts from flue gas boiler tubes in waste incinerators, Corrosion Science 50 (2008) 1627-1636.
[61] S. Jiménez, J. Ballester, Influence of operating conditions and the role of sulfur in the formation of aerosols from biomass combustion, Combustion and Flame, 4 (2005) 346-358.
[62] B. Arias, C. Pevida, F. Rubiera, J.J. Pis, Effect of biomass blending on coal ignition and bornout during oxy-fuel combustion, Fuel 87 (2008) 2753-2759.
[63] L. L. Baxter, Ash deposition during biomass and coal combustion: a mechanistic approach, Biomass and Bioenergy 4 (1993) 85-102.
[64] H. P. Nielsen, L. L. Baxter, G. Sclippa, C. Morey, F. J. Frandsen, K. Dam-Johansen, Deposition of potassium salts on heat transfer surfaces in straw-fired boilers: a pilot-scale study, Fuel 79 (2000) 131-139.
[65] A. L. Robinson, H. Junker, L. L. Baxter, Pilot-scale investigation of the influence of coal-biomass cofiring on ash deposition, Energy & Fuels 16 (2002) 343-355.
[66] H. Miettinen Westberg, M. Bystroem, and B. Leckner, Distribution of Potassium, Chlorine, and Sulfur between Solid and Vapor Phases during Combustion of Wood Chips and Coal, Energy & Fuels 17 (2003) 18-28.
[67] K. H. Andersen, F. J. Frandsen, P. F. B. Hansen, K. Wieck-Hansen, I. Rasmussen, P. Overgaard, K. Dam-Johansen, Deposit formation in a 150 MW_e utility pf-boiler during co-combustion of coal and straw, Energy & Fuels 14 (2000) 765-780.
[68] N. Otsuka, A thermodynamic approach on vapor-condensation of corrosive salts from flue gas boiler tubes in waste incinerators, Corrosion Science 50 (2008) 1627-1636.
[69] S. Jiménez, J. Ballester, Influence of operating conditions and the role of sulfur in the formation of aerosols from biomass combustion, Combustion and Flame, 4 (2005) 346-358.
[70] B.J.P. Buhre, J.T. Hinkley, R.P. Gupta, T.F. Wall, P.F. Nelson, Submicron ash formation from coal combustion, Fuel 84 (2005) 1206–1214.
[71] Experimental study of ash formation during pulverized coal combustion in O2/CO2 mixtures, Changdong Sheng , Yi Li, Fuel 87 (2008) 1297–1305
[72] In situ high-temperature phase transformation studies on pyrite, S.K. Bhargava, A. Garg, N.D. Subasinghe, Fuel 88 (2009) 988–993
[73] Iron transformations during combustion of Pittsburgh no. 8 coal, Taofang Zeng, Joseph J. Helble, Lawrence E. Bool , Adel F. Sarofim. Fuel 88 (2009) 566–572.
[74] Fine Ash Formation during Pulverized Coal Combustions, A Comparison of O_2/CO_2 Combustion versus Air Combustion**,** Changdong Sheng, Yuhong Lu, Xiangpeng Gao, and Hong Yao
[75] B. J. Skrifvars, R. Backman, M. Hupa, Characterization of the sintering tendency of ten biomass ashes in FBC conditions by a laboratory test and by phase equilibrium calculations, Fuel Processing Technology 56 (1998) 55-67.
[76] M. Zevenhoven-Onderwater, R. Backman, B.K. Scrifvars, M. Hupa, The ash chemistry in fluidized bed gasification of biomass fuels. Part I: predicting the chemistry of melting ashes and ash-bed material interaction, Fuel 80 (2001) 1489-1502.
[77] M. Aho, E. Ferrer, Importance of coal ash composition in protecting the boiler against chlorine deposition during combustion of chlorine-rich biomass, Fuel 84 (2005) 201-212.
[78] X. Wei, C. Lopez, T. von Puttkamer, U. Schnell, S. Unterberger, K. R. G.Hein, Assessment of chlorine-alkali-mineral interactions during co-combustion of coal and straw, Energy & Fuels 16 (2002) 1095-1108.